SYNTHESIS OF QUANTUM DOT-BASED FLUORESCENT SENSORS FOR DETECTION OF
ANIONIC METABOLITES AND COPPER (II) ION

Miss Nattakarn Phromsiri

จุฬาลงกรณ์มหาวิทยาลัย
CHULALONGKORN UNIVERSITY

A Dissertation Submitted in Partial Fulfillment of the Requirements
for the Degree of Doctor of Philosophy in Chemistry
Department of Chemistry
FACULTY OF SCIENCE
Chulalongkorn University
Academic Year 2021
Copyright of Chulalongkorn University

การสังเคราะห์ฟลูออเรสเซนต์เซ็นเซอร์ฐานควอนตัมดอตสำหรับการตรวจวัดเมแทบอไลต์ที่มีประจุลบ
และอิออนของคอปเปอร์ (II)

น.ส.ณัฐกาญจน์ พรหมศิริ

จุฬาลงกรณ์มหาวิทยาลัย

CHULALONGKORN UNIVERSITY

วิทยานิพนธ์นี้เป็นส่วนหนึ่งของการศึกษาตามหลักสูตรปริญญาวิทยาศาสตรดุษฎีบัณฑิต
สาขาวิชาเคมี ภาควิชาเคมี
คณะวิทยาศาสตร์ จุฬาลงกรณ์มหาวิทยาลัย
ปีการศึกษา 2564
ลิขสิทธิ์ของจุฬาลงกรณ์มหาวิทยาลัย

Thesis Title	SYNTHESIS OF QUANTUM DOT-BASED FLUORESCENT SENSORS FOR DETECTION OF ANIONIC METABOLITES AND COPPER (II) ION
By	Miss Nattakarn Phromsiri
Field of Study	Chemistry
Thesis Advisor	Assistant Professor Dr. NUMPON INSIN
Thesis Co Advisor	Assistant Professor Dr. PANNEE LEELADEE

Accepted by the FACULTY OF SCIENCE, Chulalongkorn University in Partial Fulfillment of the Requirement for the Doctor of Philosophy

⋯⋯⋯⋯⋯⋯⋯⋯⋯⋯⋯ Dean of the FACULTY OF SCIENCE

(Professor Dr. POLKIT SANGVANICH)

DISSERTATION COMMITTEE

⋯⋯⋯⋯⋯⋯⋯⋯⋯⋯⋯ Chairman

(Professor VUDHICHAI PARASUK)

⋯⋯⋯⋯⋯⋯⋯⋯⋯⋯⋯ Thesis Advisor

(Assistant Professor Dr. NUMPON INSIN)

⋯⋯⋯⋯⋯⋯⋯⋯⋯⋯⋯ Thesis Co-Advisor

(Assistant Professor Dr. PANNEE LEELADEE)

⋯⋯⋯⋯⋯⋯⋯⋯⋯⋯⋯ Examiner

(Professor Dr. THAWATCHAI TUNTULANI)

⋯⋯⋯⋯⋯⋯⋯⋯⋯⋯⋯ Examiner

(Assistant Professor Dr. MONPICHAR SRISA-ART)

⋯⋯⋯⋯⋯⋯⋯⋯⋯⋯⋯ External Examiner

(Dr. Kantapat Chansaenpak)

ณัฐกาญจน์ พรหมศิริ : การสังเคราะห์ฟลูออเรสเซนต์เซ็นเซอร์ฐานควอนตัมดอตสำหรับการตรวจวัดเมแทบอไลต์ที่มีประจุลบและอิออนของ คอปเปอร์ (II). (SYNTHESIS OF QUANTUM DOT-BASED FLUORESCENT SENSORS FOR DETECTION OF ANIONIC METABOLITES AND COPPER (II) ION) อ.ที่ปรึกษาหลัก : ผศ. ดร.นำพล อินสิน, อ.ที่ปรึกษาร่วม : ผศ. ดร.พรรณี ลีลาดี

ออกซาเลต ซิเตรต และยูเรต เป็นเมแทบอไลต์ที่มีประจุลบซึ่งเป็นผลิตภัณฑ์จากกระบวนการเมแทบอลิซึม สารเหล่านี้สามารถเป็นตัวบ่งชี้การ เกิดโรคในร่างกายมนุษย์ได้ เช่น ปริมาณออกซาเลตในปัสสาวะสามารถบ่งชี้ถึงความเสี่ยงของการเกิดนิ่วในไต และ ขระดับยูเรตในปัสสาวะก็สามารถบ่งบอกถึง ความเสี่ยงต่อการเกิดโรคเกาต์ ทางผู้วิจัยจึงมีจุดมุ่งหมายเพื่อพัฒนาการตรวจวัดเมแทบอไลต์ที่มีประจุลบโดยใช้ฟลูออเรสเซนต์เซ็นเซอร์ฐานควอนตัมดอต ร่วมกับหลักการของถ่ายโอนพลังงานฟลูออเรสเซนต์แบบเรโซแนนซ์ หรือ FRET และการวิเคราะห์แบบอัตราส่วนหรือ ratiometric เพื่อเพิ่มความไวและ เฉพาะเจาะจงต่อการตรวจวัดเมแทบอไลต์ที่มีประจุลบ

สารประกอบเชิงซ้อนของทองแดงหรือ Cu$_2$L เคยถูกนำมาใช้ร่วมกับอิโอซินวายซึ่งเป็นสารวาวแสง เพื่อตรวจจับออกซาเลต แต่ภายหลังพบว่า สารประกอบเชิงซ้อนนี้มีการตอบสนองต่อยูเรตมากกว่าออกซาเลต นอกจากนั้นแล้วในระบบการตรวจวัดที่มีควอนตัมดอตที่เป็นองค์ประกอบนั้นมีการ เสื่อมสภาพการวาวแสงเนื่องจากไอออนทองแดง จึงนำมาสู่งานวิจัย 2 หัวข้อ คือการตรวจจับยูเรตและไอออนทองแดงในน้ำ

การตรวจวัดยูเรตนั้นทำโดยใช้สารวาวแสงที่เป็นที่นิยม สองชนิด ร่วมกับสารประกอบเชิงซ้อนทองแดง อาศัยหลักการของ FRET, ratiometric และ หลักการการแทนที่อินดิเคเตอร์ เรียกว่า "ดูโอดายโพรบ – dual-dyes probe" สำหรับกลไกการการเปลี่ยนสีวาวแสงคือ สีย้อมควินินซัลเฟตที่เปล่งแสง สีน้ำเงินเป็นตัวให้พลังงานแก่ อิโอซินวาย ที่เปล่งแสงสีเขียว และในขณะเดียวกัน การวาวแสงของอิโอซินวายจับถูกดับด้วยสารประกอบเชิงซ้อนทองแดง เมื่อ ในระบบมียูเรต ยูเรตแทนที่ตำแหน่งของอิโอซินวายและอิโอซินวายจะกลับมาวาวแสงอีกครั้ง จากการศึกษาพบว่า สารประกอบเชิงซ้อนทองแดงมีการ ตอบสนองต่อไอออนปะจุลบหลัก ๆ 3 ชนิดคือ ยูเรต ออกซาเลต และซิเตรต โดยมีขีดจำกัดการตรวจจับคือ 0.0699, 0.3790 และ 1.0472 ไมโครโมลต่อลิตร ตามลำดับ ผู้วิจัยได้ออกแบบการตรวจวัดที่เฉพาะเจาะจงต่อยูเรตได้ด้วยการเจือจางของสารตัวอย่างในอัตราส่วนที่เหมาะสม พบว่าชุดตรวจนี้ให้ผลเชิงบวกใน การวิเคราะห์กับปัสสาวะสังเคราะห์และตัวอย่างปัสสาวะสังเคราะห์ของผู้ป่วยโรคเกาต์ด้วย สรุปได้ว่างานวิจัยนี้สามารถพัฒนาการตรวจวัดที่มีความว่องไวและ จำเพาะเจาะจงต่อยูเรตอีกทั้งยังง่าย สะดวก รวดเร็ว ต้นทุนต่ำ และไม่ต้องมีขั้นตอนการเตรียมสารตัวอย่างที่ยุ่งยาก นอกจากนั้นแล้วยังสามารถนำไป ประยุกต์ใช้จริงได้ในอนาคตอีกด้วย

งานวิจัยที่สอง คือ การพัฒนาการตรวจวัดไอออนทองแดงในน้ำนั้นทำโดยอาศัยหลักการของ FRET และ ratiometric ระหว่างควอนตัมดอต 2 ชนิด คือ ซิลิกอนควอนตัมดอต (ตัวให้พลังงาน) และแคดเมียมซีลีไนด์ควอนตัมดอต (ตัวรับพลังงาน) ระบบนี้เรียกว่า "mixed-QDs probe" ในระบบนี้ สารละลายวาวแสงสีเหลืองเขียว และเมื่อมีไอออนทองแดงในระบบ สารละลายจะเปลี่ยนเป็นสีฟ้าของซิลิกอนควอนตัมดอต ซึ่งเป็นผลมาจากไอออนของ ทองแดงที่มีต่อพื้นผิวควอนตัมดอตและทำการศึกษาโดยใช้ผลกระทบต่อควอนตัมดอตโดยอาศัยเทคนิคเอ็กซ์เรย์โฟโตอิเล็กตรอนสเปกโตรมิเตอร์ (XPS) พบว่า สาเหตุของการเปลี่ยนสีจากสีเหลืองเขียว ไปเป็น ฟ้า ของสารละลายนั้น เกิดจากพื้นผิวของแคดเมียมซีลีไนด์ควอนตัมดอตถูกรบกวนด้วยไอออนทองแดงจึงไม่ สามารถวาวแสงได้อีก นอกจากนั้นพบว่าระบบนี้มีความไวและเจาะจงต่อไอออนทองแดงมากเมื่อเปรียบเทียบกับไอออนที่มีประจุบวกชนิดอื่น ๆ มีขีดจำกัดการ ตรวจจับอยู่ที่ 3.89 นาโนโมลต่อลิตร และการเปลี่ยนแปลงของสีจากสีเหลืองเขียวไปเป็นฟ้าของ mixed-QDs probe สามารถนำไปสู่การตรวจจับทองแดง ไอออนในน้ำได้จริง

สาขาวิชา	เคมี	ลายมือชื่อนิสิต ....
ปีการศึกษา	2564	ลายมือชื่อ อ.ที่ปรึกษาหลัก ....
		ลายมือชื่อ อ.ที่ปรึกษาร่วม ....

5872808823 : MAJOR CHEMISTRY

KEYWORD:

Nattakarn Phromsiri : SYNTHESIS OF QUANTUM DOT-BASED FLUORESCENT SENSORS FOR DETECTION OF ANIONIC METABOLITES AND COPPER (II) ION. Advisor: Asst. Prof. Dr. NUMPON INSIN Co-advisor: Asst. Prof. Dr. PANNEE LEELADEE

Oxalate, citrate, and urate are the anionic metabolites that are the products of the metabolism pathway of living organisms. The high level of these anionic metabolites is related to the diseases. For example, the excess amount of oxalate ions in urine indicates the risk of kidney stones, while the level of citrate can suggest the risk of cancer. The level of urate in urine is related to the risk of gout. The detection of these anionic metabolites is significant and still remains a challenge. Thus, this work aims to develop the more sensitive and selective fluorescence sensing of oxalate in aqueous-based by using dinuclear copper(II) complex, Cu_2L with eosin Y dyes that was reported as a fluorescence sensing for oxalate in the water earlier with quantum dots (QDs). However this complex shows a higher sensitivity to urate rather than oxalate. To improve the sensitivity and selectivity of the sensing system, the ratiometric and fluorescence resonance energy transfer (FRET) was applied to the new approach. To fabricate the ratiometric and FRET system of eosin Y to QDs, the blue-emitting QDs are required. Unfortunately, the blue-emitting aqueous-based QDs are mostly quenched by Cu^{2+} ions. Hence, it has become the two fluorescence sensing projects which are the detection of urate and Cu^{2+} ions. The first naked-eyes probe called the "dual-dyes probe" was constructed for urate detection. According to the ratiometric fluorescence method and FRET, this dual-dyes system has an indicator displacement assay (IDA) for the fluorescence turn-on mechanism. Blue-emitting quinine sulfate dyes is a donor and green-emitting eosin Y is an acceptor in the FRET system. The energy transfer was confirmed by fluorescence titration. Eosin Y also acts as an indicator in IDA with the Cu_2L as a host. Dual-dyes probe responds to 3 main anions which are urate, oxalate, and citrate. The detection limit are 0.0699, 0.3790, and 1.0472 µmol L^{-1}, respectively. According to the urate, oxalate, and citrate anions concentration found in the urine are 1.49-4.46, 0.7-2.3, and 0.13-0.46 mmol L^{-1} [1, 2]. With the optimal dilution factor, we are able to obtain the selective probe for urate detection and it can be operated in the synthetic urine and gout patient's mimic synthetic urine samples. This approach is simple, convenient, fast, sensitive, selective, and low-cost without any pretreatment step and provides the obvious fluorescence color changing from blue to green in the presence of urate. This obvious change in the fluorescence color would lead to the opportunity of the onsite test kit for the preliminary screen of gout. The second probe is a mixed-QDs probe for the detection of Cu^{2+}. Although, the Cu^{2+} ion is one of the essential ions for humans, the excessive amount of it is toxic. Additionally, Cu^{2+} is a toxic heavy metal in the environment. The facile, simple, sensitive, and selective probe for Cu^{2+} detection was fabricated by using the ratiometric system and FRET between 2 different types of QDs. There are blue-emitting Si QDs (donor) and green-emitting CdSe QDs (acceptor). The mixed-QDs probe has a yellow-green fluorescence color. The FRET between Si QDs and CdSe QDs was confirmed by the fluorescence titration and time-resolved fluorescence. The fluorescence color chang from the yellow-green of the mixed-QDs to the blue-emission of the only Si QDs was observed in the addition of Cu^{2+}. The X-ray photoelectron spectrometer (XPS) technique was used to study the effect of Cu^{2+} on to QDs surfaces. The change mainly depends on the quenching of CdSe QDs surfaces. The mixed-QDs probe shows a very low detection limit of 3.89 nmol L^{-1} and has a high selectivity toward Cu^{2+} ions compared to Co^{2+}, Fe^{3+}, Zn^{2+}, Al^{3+}, Mg^{2+}, Cr^{3+}, Ba^{2+}, Li^+, Ca^{2+}, Sr^{2+}, Ag^+, Na^+, Ni^{2+}, K^+, Cd^{2+}, Pb^{2+}, Mn^{2+}, and Hg^{2+} ions.

Field of Study:	Chemistry	Student's Signature ....
Academic Year:	2021	Advisor's Signature ....
		Co-advisor's Signature ....

ACKNOWLEDGEMENTS

Firstly I would like to appreciate Assistant Professor Dr. Numpon Insin, my thesis advisor, Professor Dr. Pannee Leeladee, my thesis coadvisor, and Associate Professor Andrew B. Greytak for their advices, motivation and the valuable assistance to achieve this thesis.

For the useful comments and suggestions, I would like to thanks my thesis committee, Professor Dr. Thawatchai Tuntulani, Assistant Professor Dr. Monpichar Srisa-Art, and Dr. Kantapat Chansaenpak. Also for seminar committee class 2022, Associate Professor Dr. Boosayarat Tomapatanaget, Assistant Professor Dr. Puttaruksa Varanusupakul, Professor Dr. Sanong Ekgasit, and Dr. Chanat Aonbangkhen. And Associated Professor Dr. Jeerus Sucharitakul for his kindness assistance my work.

In addition I would like to spacial thanks all of my colleagues in NI's group, Supramolecular Chemistry Research Unit, SCRU group and ABG's group for their emotional & knowledgth support and the huge helpful advices for both life and study espectially, Miss Natthaya Theppanao, Miss Padtaraporn Chunhom, Mr. Chonnavee Maneepunti, Miss. Wishulada Injumpa, Miss Chalatan Saengruenggrit, Dr. Kamonlatth Rodponthukwaji, Miss. Ajirawadee Suwanchan, Dr. Tossapong Phuangburee, Mr. Sakiru L. Abiodun, Dr. Fiaz Ahmed, Mr. Nuwanthaka Jayaweera, Dr. John Dunlap, Dr. Preecha Kittikhunnatham, and Dr. Megan Gee. Also other lab group particularly, Miss Pawittra Chaibuth, Dr. Kingkarn Pungjunun, Mr. Kriangsak Faikhruea, and Miss. Kotchakorn Supabowornsathit.

The other spacial group, I would to express my greatest gratitude to my family who gave me everything in my life and friends for their love, kindness and encouragement at all times.

Nattakarn Phromsiri

TABLE OF CONTENTS

LIST OF ABBREVIATIONS

QDs	-	Quantum dots
L	-	Bis-p-bylylBISDIEN ligand
Cu_2L	-	Dinuclear copper (II) complex of Bis-p-bylylBISDIEN ligand
XPS	-	X-ray Photoelectron Spectrometer
FT-IR	-	Fourier Transform Infrared
FETEM	-	Field emission transmission electron microscope
SAED	-	Selected Area Electron Diffraction
EDS	-	energy-dispersive X-ray spectroscopy
DLS	-	Dynamic light scattering
UV-VIS	-	Ultraviolet-visible
Abs	-	Absorption
Emit	-	Emission
L	-	Liter
mL	-	Milliliter
g	-	Gram
n	-	Nano
μ	-	Micro
M	-	Molar (mol/L)
UA	-	Uric acid/urate
OX	-	Oxalate
Cit	-	Citrate
en	-	Ensemble

LIST OF FIGURES

LIST OF TABLES

CHAPTER I

INTRODUCTION

1.1 Statement of problem

Anionic metabolites are products from the metabolism pathways of animals, plants, and bacteria. Oxalate, citrate, and urate are the anionic metabolites in the human body. These anionic metabolites become well-known bio-markers since the levels of these anions are related to the risk of many diseases. With early notice of this abnormal anionic metabolite level, we can avoid and adjust our behaviors for better health.

Thus, the determination of anionic metabolites gets a lot of interest. A ratiometric fluorescence sensor is one of the methods that is mostly applied for anionic metabolites detections. The fluorescence technique provides a low cost, sensitive, selective, and easy-to-operate method, and it can be of a naked-eye detection device. In addition, the effect of instrument, sample media, and the probe concentration were eliminated.

There are a number of reports on using FRET system to develop chemosensors and biosensors. As the naked-eye detection ability of fluorescence method, it could be developed to obvious fluorescence color changing from one to another color by the fluorescence resonance energy transfer (FRET) between two fluorophores, instead of just variation in fluorescent intensity.

A dinuclear copper (II) complex of a Bis-p-bylylBISDIEN ligand was reported as a promising urate detection via the fluorescence indicator displacement assay (IDA) of commercial dyes and urate by Hontz. D. [1]. This dinuclear copper (II) complex is selective to urate, oxalate, and citrate over other important anions in biological samples. Under the optimized condition of the detection method, we can eliminate the effects from oxalate and citrate in the urine samples.

In order to obtain a simple, fast, sensitive and selective method with possibility for the naked-eyes device for the determination of urate in an aqueous solution, the combination of FRET and IDA in a ratiometric fluorescence sensor would be a great idea.

Unfortunately, our chosen donor fluorophore which is quantum dots (QDs) is sensitive to Cu^{2+} ions as the quench of QDs fluorescent was observed when exposed to Cu^{2+}. From this observation, another application on the determination of Cu^{2+} ions in an aqueous solution with the QDs-based ratiometric fluorescence sensor was investigated. Although Cu^{2+} ions are essential to the human body but the excessive amount of Cu^{2+} also causes a problem for the human body. Moreover, it causes environmental pollutants, especially in water.

Thus, here we report new ratiometric fluorescence sensors for the detection of urate by the dual-dyes system and detection of Cu^{2+} ions by the mixed-QDs system with the single, sensitive, selective, and easy-to-operate method. These approaches for both urate and Cu^{2+} have potential to become the naked-eyes device for on-site use upon the further engineering modification technique.

1.2 Objectives of thesis

i) To fabricate fluorescence-based sensing for the selective detection of anionic metabolites in water

ii) To fabricate a new ratiometric fluorescence sensor for Cu^{2+} detection by quantum dots-based probe system with the fluorescence resonance energy transfer.

1.3 Scope of thesis

This thesis works on 2 main subjects which are

i)   Detection of oxalate, citrate, and urate in aqueous solution using a
dual dyes system cooperated with the indicator displacement assay and
ratiometric fluorescence titration

ii)   Detection of copper (II) ions in an aqueous system using a mixed QDs-
probe as a ratiometric fluorescence sensor

1.4 The benefits of this thesis

i)   Obtain a probe with the ratiometric fluorescence titration based on
the indicator displacement assay for selective urate detection in a synthetic
urine sample.

ii)   Obtain the quantum dots-based ratiometric fluorescence sensor for
selective Cu^{2+} detection in aqueous solution.
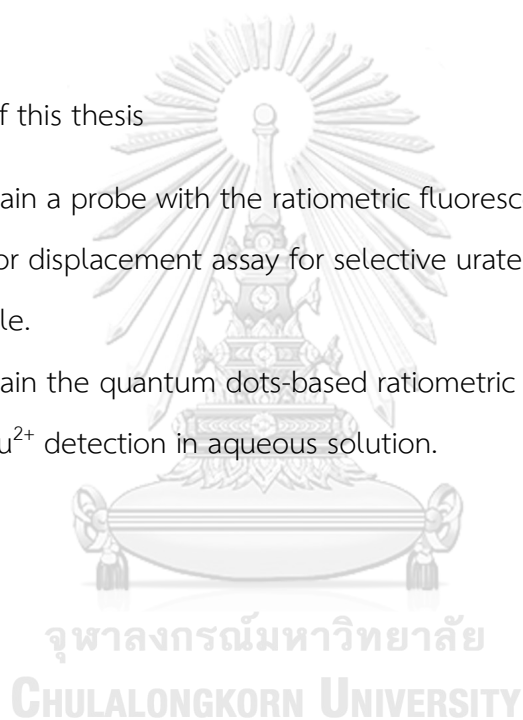
CHAPTER II

THEORY AND LITERATURE REVIEW

2.1 Quantum dots, QDs

Quantum dots or QDs are colloidal semiconductor nanomaterials with zero-dimension. The quantum confinement effect [2] in the nano size of quantum dots causes unique chemical and physical properties. The promising properties of QDs are the color/size-tunable properties with broad absorption and narrow emission spectra(Figure 2.1). Normally, the absorption spectra of QDs extend from the ultraviolet to visible range according to the QDs size [3] (Figure 2.2.)
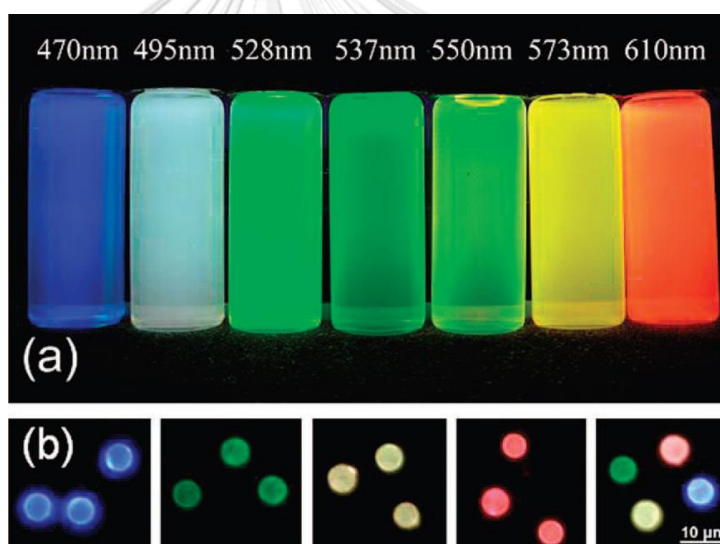
Figure 2.1 The tunable emission colors of CdSe QDs with different sizes in n-hexane [4].

The color, size, and shape of QDs play a crucial role in the nanotechnology study. These properties depend on many factors including the chemical component, the ratio of the elements, and the synthesis method. There are various types of QDs that were reported nowadays including CdSe, CdTe, ZnSe/ZnS, CuInSe, InP, carbon dots, silicon QDs, etc.
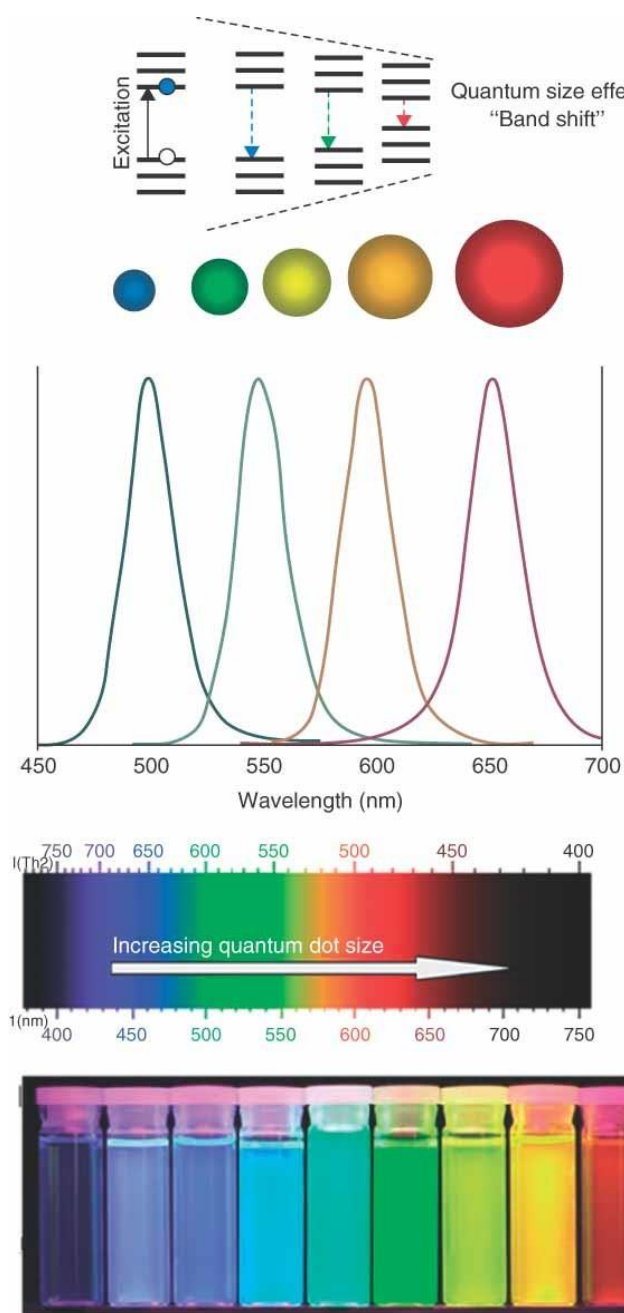
Figure 2.2 The illustration of the change in size/color of QDs and their electronic configuration structure.

Mostly, QDs were prepared by high-temperature synthesis in an organic solvent via the organometallic synthesis pathway [5]. In many applications that work in an aqueous solution, especially in the biological field, the non-aqueous-based QDs will need further surface modification [6] to allow QDs dispersed in the water. This process

involved surface functionalization. This surface modification method is usually complicated and difficult to operate and reduces the quantum yield of QDs.

There are direct aqueous-based QDs synthesis approaches such as one-pot synthesis including the hot-injection method [7-8], microwave method [9-10], and hydrothermal method [11]. All these methods are less complicated and still provide a high quantum yield.

These unique optical and physical properties of QDs give QDs significant advantages over traditional organic dyes in various research fields such as bioimaging and bio-sensor, as compared in Table 2.1
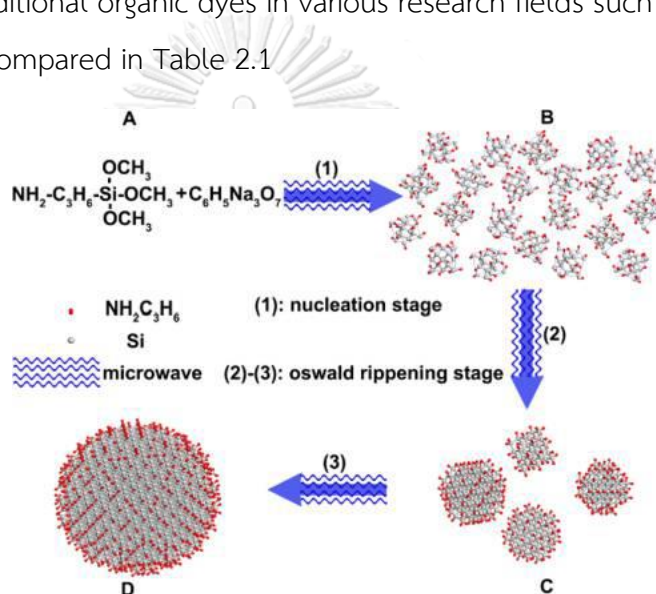
Figure 2.3 The schematic illustrates the one-pot synthesis of Si QDs with the microwave assisted [10].
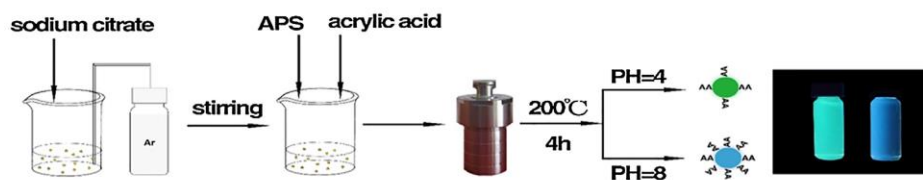
Figure 2.4 The schematic illustrates the preparation of Si QDs via a hydrothermal method [11].

Table 2.1 A summary of the characteristic comparison between quantum dots and traditional organic dyes.

Properties	Quantum dots (QDs)	Organic dyes	Ref.
Absorption spectra	Broad	Narrow	12
Emission spectra	Narrow in bandwidth 20 – 40 nm	Broad, asymmetric, and tail	12
Stokes shift	300 – 400 nm	Less than 100 nm	13
Quantum yield	40 – 90%, depending on buffer and surface modification	Variable -depends on the chosen fluorophore	14
Fluorescence life time	20 – 50 ns	Few nanoseconds	15
Photostability	Strong resistance to photobleaching	Variable - depends on chosen fluorophore	14

2.1.1 CdSe QDs

CdSe QDs are the most common nanoparticles in Type II-VI semiconductors. There are many CdSe QDs synthesis methods in both organic and aqueous solvents. Water-soluble CdSe QDs are mainly made up of 2 strategies i) surface modification: ligand exchange of hydrophobic CdSe QDs [16-17], ii) initially synthesizing CdSe QDs in an aqueous system [18]. The most common ligands for water-soluble CdSe QDs is the thiol and carboxyl group-containing ligands [8, 18-19]. As the unique optical properties of QDs, CdSe QDs were widely used in many applications, such as optical sensor [19-21], solar cell [22], fluorescence tagging [23], and light-emitting diodes [24].

2.1.2   Si QDs

Si QDs are colloidal nanocrystals made from Si sources. The well-known stabilizers for aqueous Si QDs are trisodium citrate, acrylic acid, and glucose [10, 25-26]. The well-known silicon sources are silane derivatives. Since the majority of Si QDs is silicon, which is low toxicity, and the surface of Si QDs has the active functional groups, Si QDs are biocompatible, low toxic, and have surface painting ability.

There are 2 main synthesis strategies called "top-down" and "bottom-up" [25].

In the top-down method, water-soluble Si QDs were prepared from a hydrophobic silicon nanomaterial of a large size such as silicon oxide powder, silicon nanowires, and bulk silicon. Then, the surface modification is required to make water dispersed QDs by using acids e.g. HCl, HF, and HNO_3. This surface modification is not only toxic, but also causes chemical instability and damages to the optical property of QDs, resulting in the reduction of quantum yield.

On the other hand, the bottom-up approach has a variety of syntheses including the use of silicon hydride source, hydrothermal method, and microwave irradiation. This bottom-up strategy can be directly prepared in aqueous solution and generally provide the blue-emitting QDs, which are difficult to obtain from the other type of QDs. Moreover, these Si QDs show a high quantum yield, with the non-toxic and cheap regents and with the simple methodology in preparation.

2.2 Förster/fluorescence resonance energy transfer, FRET theory

Förster resonance energy transfer or fluorescence resonance energy transfer or FRET was first discovered by a German scientist named "Theodor Förster" [27]. This is a non-radiative transition of energy between two materials or molecules, called donor (D) and acceptor (A), on a FRET pair. The transfer of the energy between the donor and the acceptor resulted from long-range dipole-dipole interaction and does not include photon emission. There are a few criteria for FRET to occur: i) the overlapping of the emission of a donor to the absorption energy of an acceptor is bigger than

30% (Figure 2.5), ii) the distance between donor/acceptor is required to be close to one another to allow the energy transfer, typically 1-10 nm, iii) the transition dipole of donor/acceptor is required to be parallel to each other, iv) the fluorescence lifetime of the donor have to be longer than the duration time of the energy transfer [28-29]. FRET efficiency was described as equation 1 [30].

$$E = \frac{k_{D-A}}{k_{D-A}+k_D} = \frac{R_0^6}{R_0^6+r^6} = 1 - \frac{I_{DA}}{I_D};$$

equation 1.

where

E = FRET efficiency

k_{D-A} = the donor decay rate in the presence of an acceptor

k_D = the donor decay rate in the absence of an acceptor

R_0 = the donor and acceptor distance at FRET efficiency is 50%

r = the actual donor and acceptor distance

I_{DA} = the integrated emission intensity of the donor in the presence of an acceptor

I_D = the integrated emission intensity of the donor in the absence of an acceptor

The FRET process initially starts when the incident light excites electrons of the donor fluorophore from the ground state to the excited state. While the relaxation of the donor (D), the relaxing energy is transferred to the nearby chromophore or fluorophore acceptor (A), Figure 2.6 [28]

$$D + hv \rightarrow D*$$
$$D* + A \rightarrow D + A*$$
$$A* \rightarrow A + hv'$$
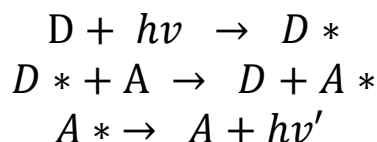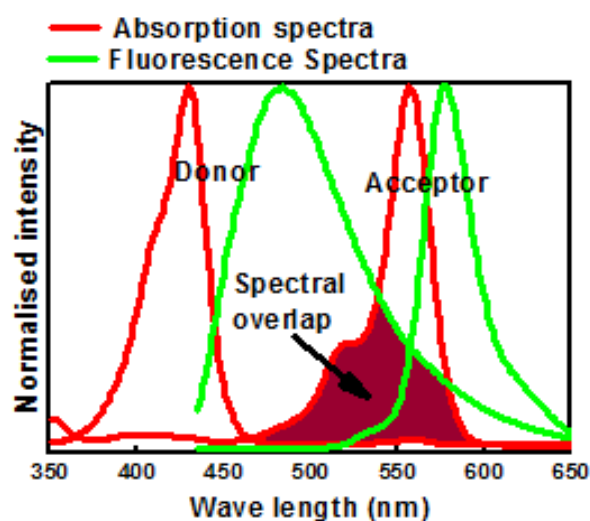
Figure 2.5 Absorption and fluorescence spectra of an ideal donor and acceptor pair [28].
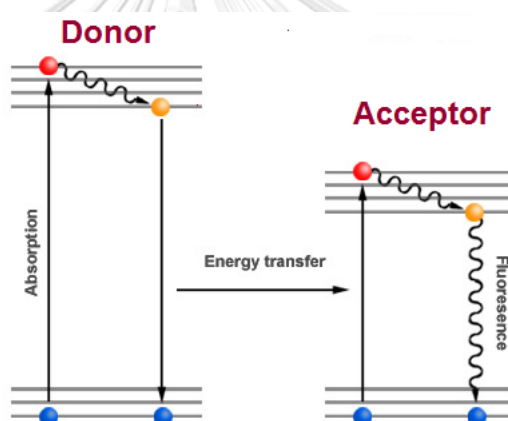
Figure 2.6 Jablonski diagram presenting Förster resonance energy transfer [28].

2.3 Indicator displacement assays, IDAs

Indicator spacer receptor (ISR) is a traditional approach for chemosensors, but this assay requires the direct covalent bond between host and indicator. Therefore, it is difficult to synthesize the direct attached host-indicator materials, while the indicator displacement assay is much easier to generate. Thus, IDA becomes the most popular approach for chemosensing [20, 31-32].

The indicator displacement assay (IDA) mechanism is the replacement of an indicator by an analyze on the host, Figure 2.7. The interaction between the host to

the indicator is easy to generate because it is a non-covalent interaction such as electrostatic interaction, and H-bonding interaction. Moreover, IDAs can be applied for both colorimetric and fluorimetric detections relying on the indicator and can be operated on both aqueous and non-aqueous systems.
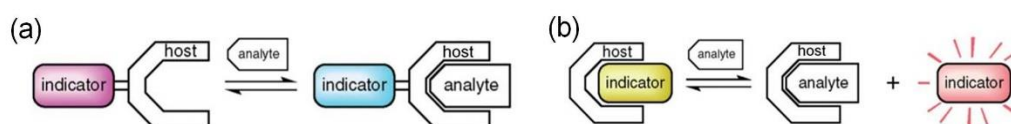
Figure 2.7 The schematic of the indicator spacer receptor chemosensing assay, ISR (a), and indicator displacement assays, IDAs (b) [33].

CHAPTER III

QDs-based detection of oxalate ions

Oxalate ion is one of the anionic metabolites. It is a nutrient for humans and is found in several foods. There is no enzyme for oxalate digestion, so the excess amount of oxalate ions was excreted by the kidney via urine [34]. Insoluble calcium oxalate crystals were crystallized by the excess of oxalate ions and calcium ions in the body. The calcium oxalate crystals may accumulate in the body and develop kidney stones and bladder stones diseases [35]. The quantitative information of oxalate ions that were excreted in urine refers to the possibility of kidney stones and bladder stones diseases. Therefore, the detection of oxalate ions is significant. There are several studies on oxalate sensing based on fluorescence methods [36-39]. Although the fluorescence technique is simple, quantitative information of oxalate ions depends on many factors, such as probe concentration, media, and instrument factors. To avoid these limitations, a ratiometric fluorescence system was applied. Instead of fluorescence intensity changing, the obvious fluorescence color changing is developed by the fluorescence resonance energy transfer (FRET). A dinuclear copper(II) complex (Cu_2L) was first reported as a host in indicator displacement assays (IDAs). It worked with eosin Y (indicator) for oxalate ions detection [36]. Their work provides a sensitive and selective method for oxalate ions sensing. Hence, we will develop a fast, simple, sensitive, selective, easy-to-operate method, and cloud be a naked-eyes device for oxalate detection by all of these concepts, including ratiometric fluorescence method, FRET, and IDAs of dinuclear copper(II) complex. Quantum dots are good donor candidates in FRET because of their tunable size, high photostability, and high quantum yield.

In summary, a new oxalate sensing approach consists of 3 main materials, which are QDs (donor), eosin Y (acceptor and indicator), and Cu_2L. Eosin Y has dual duties, which are an acceptor that accepts the energy from QDs and a turn-on indicator in IDAs. In all systems, the fluorescence of eosin Y was quenched by Cu_2L, the only QDs

provide the fluorescence. With the presence of oxalate ions, oxalate will replace eosin Y in the Cu_2L host and let free eosin Y to the system according to IDAs. This free eosin Y can accept the energy from QDs and emit their energy. The whole of this process provides the naked-eyes detection by color changing from blue of QDs to the green of eosin Y.

ZnSe/ZnS [40-42] and Si QDs [9-10, 25-26] are blue-emitting non-toxic aqueous-based quantum dots that have a matched emission energy to the absorption energy of eosin Y. Even ZnSe/ZnS QDs are a good donor for eosin Y, but it is not stable in Cu^{2+} containing environment. Their fluorescence emissions were diminished as shown in Figure 3.1 and Figure 3.2. While Si QDs are stable in a Cu^{2+} containing system, they interfere the oxalate detection as shown in Figure 3.3. It is because the stabilizing ligand of Si QDs is citrate ions. Citrate ions were reported as a sensitive anion for Cu_2L by Hontz. D. et. al. in 2020 [1]. They have a further study on the detection of the other anionic metabolite including urate and citrate. They found that this complex more sense to urate than oxalate and citrate. For this reason, the detection of urate and citrate has been studied in this thesis.
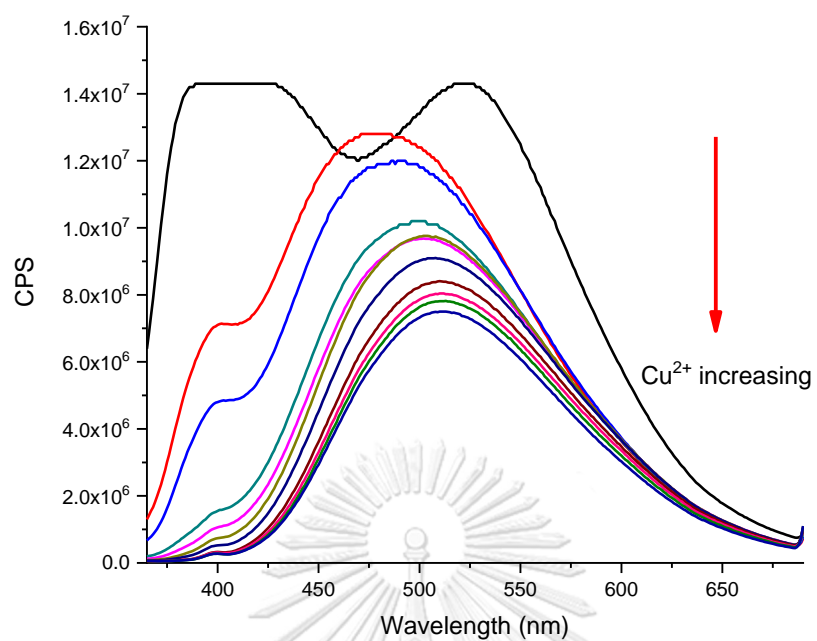
Figure 3.1 The flurescence spectras of ZnSe/ZnS in the addition of Cu^{2+} ions.
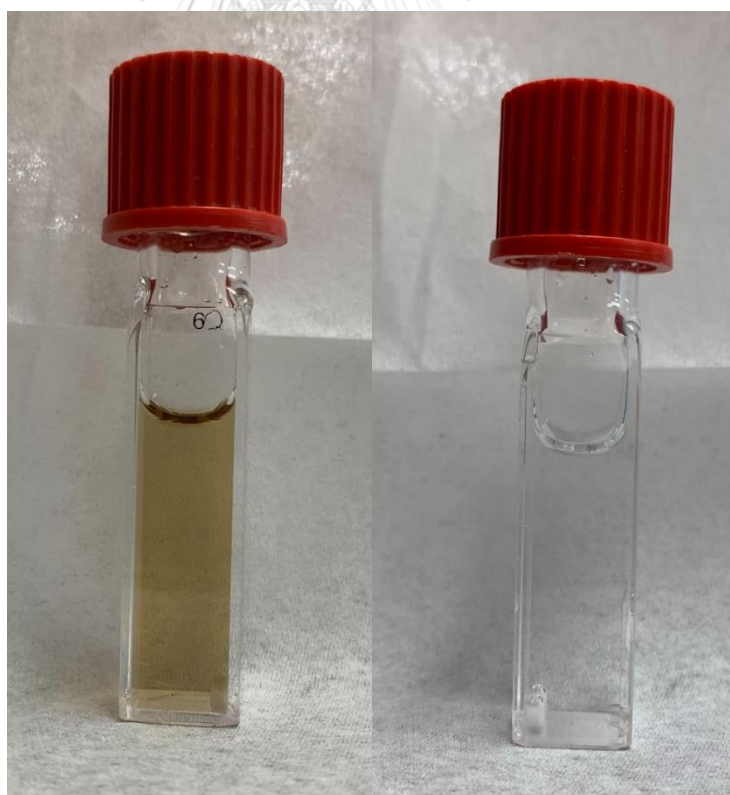
Figure 3.2 ZnSe/ZnS QDs in the presence of Cu^{2+} ions (left), ZnSe/ZnS QDs (right).
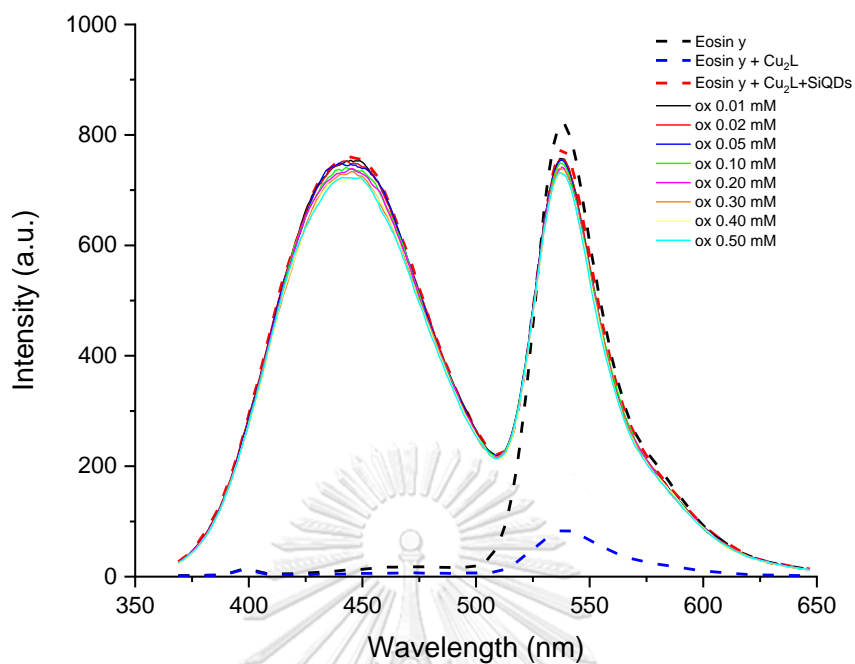
Figure 3.3 The fluorescence spectra of eosin Y with Cu_2L and Si QDs in the addition of oxalate ions.

CdSe QDs are well known as Cu^{2+} sensitive materials with a very low detection limit in an aqueous solution [17, 43]. Meanwhile, it is very sensitive to Cu^{2+}, but lack of the selectivity towards Cu^{2+} compared to some metals like Hg^{2+} and Ag^+ [44]. The previous study showed that Si QDs are stable in Cu^{2+} containing condition. Moreover Si QDs were reported as a metal sensor that resist to Cu^{2+} ion [45, 46] With the size/color-tunable CdSe QDs, it can be designed into another Cu^{2+} sensing system with the ratiometric fluorescence-based QDs method.

CHAPTER IV

The detection of uric acid in an aqueous base system by using a FRET-based dual-dye sensor.

Authors: Nattakarn Phromsiri[a], Pannee Leeladee[a], Numpon Insin[a,b]*

a Department of Chemistry, Faculty of Science, Chulalongkorn University, Thailand

b Research Unit in Integrative Immuno-Microbial Biochemistry and Bioresponsive Nanomaterials, Department of Microbiology, Faculty of Dentistry, Chulalongkorn University, Pathumwan, Bangkok, Thailand

Abstract

We reported a new ratiometric fluorescence and naked-eye detection of urate in aqueous solution and synthetic urine with a simple, convenient, fast, sensitive, selective, and low-cost method without any pre-treatment step. This probe was constructed from three main components: eosin Y, quinine sulfate, and a dinuclear copper (II) complex, Cu_2L with the cooperation of fluorescence resonance energy transfer from quinine sulfate to eosin Y and the indicator displacement assay of eosin Y by urate on the Cu_2L. The probe fluorescence color was converted from blue to green by the three sensitive anions: urate, oxalate, and citrate with the limit of detection of 0.0699, 0.3790, and 1.0472 µmol L^{-1}, respectively. The selectivity of this probe was studied over the varieties of dicarboxylate ions and the urine ions components: terephthalate, malonate, fumarate, succinate, citrate, carbonate, urate, ascorbate, oxalate, phosphate, maleate, sodium sulfate, sodium chloride, magnesium phosphate, ammonium chloride, creatinine, sodium dihydrogen orthophosphate, and di-potassium hydrogen phosphate. Under the optimized condition, this approach can

distinguish the urate from the other ions and worked well in differentiation of samples of normal synthetic urine and the one of hyperuricemia patient mimics.

Keywords: uric acid, sensor, ratiometric fluorescence, fluorescence resonance energy transfer.

1. **Introduction**

Uric acid, UA, is the end-product of the nucleotide catabolic pathway in the human body. It is well-known as a biomarker in human body fluid; urine and serum [27]. With change in diet consumption, the number of abnormal levels of the uric acid patient has grown. The normal concentration of urate in urine is 1.49-4.46 mM, oxalate is 0.7-2.3 mM and citrate is 0.13-0.46 mM [29, 43]. The excessive uric acid level or hyperuricemia represents the risk or indication of many diseases [27, 44-47] including gout, artheophlogosis, hypertension, type II–diabetes, metabolic syndrome, arthritis, leukemia, kidney stone chronic nephropathy and Lesch–Nyhan syndrome.

So far, there are various methods for the detection of urate in biofluids reported with rapid and reliable methods including fluorescence [27, 48], UV–VIS absorption [47], colorimetry [49-51], enzymatic [27, 49, 52], paper-based technique [50], capillary electrophoresis [53], chromatography [54], electrochemistry [55], etc. Fan Li, *et.al.* [49] developed a visual and colorimetric sensor for urate in human fluids using the chitosan stabilized gold nanoparticles (Ch-Au NPs), uricase, and 3,3',5,5'-tetramethylbenzidine (TMB) with the limit of detection of 0.04 µmol L^{-1} at pH 8.5 with the 37 °C incubation. Homa Rezaei, *et.al.* [47] also used gold nanoparticles (Au NPs) to fabricate the colorimetric urate sensor based on the localized surface plasmon resonance (LSPR) of Au NPs. The LOD of this work is about 0.2 mg L^{-1} (1.19 µmol L^{-1}) at pH 4.5. Tiliang Zhang, *et.al.* [48] reported the positive charge CdTe QDs with 2-mercaptoethylamine as a stabilizing ligand for the fluorimetric detection of

urate. The detection limit of this approach is 0.1030 µmol L^{-1} in an aqueous solution and pH = 5.6. However, for the daily inspection in both the clinical medicine and at-home diagnosis of an excessive amount of urate in the urine, a convenient, sensitive, selective, fast, novel, and low-cost approach is in need to be developed.

Cu$_2$L is a dinuclear copper (II) complex formed by Cu(II) ions and Bis-p-bylylBISDIEN ligand that has been investigated for its selectivity to certain dicarboxylat anions. Cu$_2$L was first reported by Lui Fabbrizzi, *et. al*. [56] for the detection of pyrophosphate in aqueous. Min Hu and Guoquiang Feng [36] published the fluorimetric detection of oxalate in water with the advantage of this Cu$_2$L and claimed that their system is sensitive and selective to oxalate over the various types of dicarboxylate ions. However, Hontz, D., *et.al*. [1] reported a greater fluorescence response in the indicator displacement assay (IDA) of urate and oxaloacetate, and citrate than oxalate. To develop a new urate sensor in aqueous and further applying in the real sample or the urine test, the selectivity of the probe to urate and the effect from the complex and colored samples need to be solved.

Here, we reported a new ratiometric dual-dye system with the fluorescence resonance energy transfer (FRET) and indicator displacement assay (IDA) concepts for urate detection in aqueous solution and synthetic urine with a convenient, sensitive, selective, fast, novel, and low-cost approach called "dual-dye probe". Two commercial dyes: green-emitting eosin Y (acceptor) and blue-emitting quinine sulfate (donor) were investigated for their FRET efficiency and the construction of a ratiometric sensing system. Eosin Y has 2 functions which are an acceptor in FRET and an indicator in the IDA. The role of IDA is the turn-off/on of fluorescence signal of eosin Y (indicator) with the binding to the specific dinuclear copper(II) complex, Cu$_2$L (host). The fluorescence of eosin Y would be slightly recovered by the addition of urate. With these components, the dual-dye system could enable the detection of urate with high selectivity in the high interference and complicated specimens such as biofluids without any pretreatment steps.

2. Experimental

2.1 Chemicals

All chemicals, reagents, and solvents were used without further purification. Quinine sulfate (99%), N-[2-Hydroxyethyl]piperazine-N'-[2-ethane-sulfonic acid or HEPES (> 98%), sodium borohydride (≥ 98%), creatinine (≥ 99%), sodium fumarate dibasic (≥ 99%). sodium malonate (≥ 99%), sodium succinate dibasic hexahydrate and maleate standard solution were purchased from Sigma-Aldrich. Tetrabromofluorescein or eosin Y (>99%), Terephthalaldehyde (> 98%), and diethylenetriamine (>98%) are from TCI. Uric acid (≥ 99%), di-potassium hydrogen phosphate (≥ 98%), copper(II) nitrate trihydrate (99.999%), and hydrobromic acid 48 wt.% in H_2O (≥99.99%) are from Merck. sodium dihydrogen orthophosphate (99%), sodium chloride (99%), sodium oxalate (99%), sodium sulfate anhydrous (99%), tri-sodium citrate (99%) and sodium carbonate anhydrous (≥ 99%) are from Univar. Calcium chloride (99%), magnesium sulfate hydrate (99%), L-ascorbic acid (99%) are from Unilab. Urea (99%) is from Vertec. Ammonium chloride (≥ 99%) is from Fluka. All solvents: methanol, dicholomethane, ethanol, acetronitrile, diethyl ether, and chloroform was purchased from ACL lab scan. The Ultrapure water is used throughout the Milli-Q pure system, Millipore.

2.2 Instrumentation

Absorption spectra were recorded using a UV - HP 8453, UV-VIS spectrophotometer. Fluorescence spectra measurements were done with a Cary Eclipse Fluorescence spectrophotometer at 330 nm excitation. PerkinElmer, EnSight multimode microplate reader was used to analyze fluorescence intensity in the selectivity study with the excitation wavelength at 330 nm. Elemental analysis was analyzed using THERMO FLASH 2000 CHNS/O Analyzers. Mass analysis was measured

by high resolution microOTOF-Q II mass spectrometer, Bruker. H[1]-NMR spectra were obtained from JEOL JNM-ECZ500R/S1.

2.3 Materials and syntheses and characterization

2.3.1 Synthesis of bis-p-xylylBISDIEN macrocyclic ligand, L

Macrocyclic ligand was synthesized following the previous report[57]. Briefly, 0.0090 mol of terephthalaldehyde in 150 mL anhydrous acetonitrile was added dropwise to diethylenetriamine, DIEN, solution (0.009 mol DIEN in 280 mL CH_3CN) for 1.5 h with vigorous stirring at room temperature. After 24 h of stirring, the white precipitated solid was filtered and washed with diethyl ether and recrystallized in ethanol. Then the reduction of this white crystal took place at 45°C using 2.5 g of sodium borohydride in anhydrous methanol. After 1 h of stirring, the solution was cooled and filtered then evaporated until dry. The dispersed solution of the product in 10 mL of water was extracted by dichloromethane. Sodium sulfate was added into the organic phase to remove the water before filtered out. After the evaporation of the organic phase, the product was dispersed in 100 mL of ethanol. The white precipitate was immediately formed upon addition of 10 mL 48% hydrobromic acid. The white solid ligand was filtered and washed by the mixed solution of ethanol and diethyl ether. Finally, the final product was recrystallized in ethanol This ligand product was characterized using ^{1}H-NMR and mass spectrometry. ^{1}H-NMR (500 MHz, D_2O, 298K): δ(ppm) = 3.31 (m, 8H, NH-CH_2), 3.43 (m, 8H, NH-CH_2), 4.39 (s, 8H, benzene-CH_2), 7.58 (s, benzene). Calculation m/z of L, $[C_{24}H_{38}N_6]^+$ is 410 (100.0%), 411 (26.0%), 412 (2.7%), 411 (2.2%).

2.3.2 Synthesis of dinuclear copper (II) complex, Cu_2L or CuCpx

Dinuclear copper(II) complex was synthesized following Fabbrizzi, L., *et. al*.'s report[56]. The complexation of Cu_2L was carried out in methanol solution. After 30

min reflux of the mixed solution of copper(II)nitrate and ligand solution, the blue solid was obtained. The blue precipitate was filtered and washed with cold methanol. Cu_2L was characterized using elemental analysis and mass spectrometry. Calculated m/z of Cu_2L is 22 (100.0%), 724 (89.1%), 723 (26.0%), 725 (23.1%), 726 (19.9%), 727 (5.2%), 723 (3.3%), 724 (3.2%), 726 (2.4%), 724 (1.8%), 726 (1.6%), 725 (1.6%), 725 (1.3%). Found: 722.1583. Anal. Calc. for $[C_{24}H_{38}Cu_2N_9O_9]^+$: C 39.83, H 5.29, N 17.42%. Found: C 39.69, H 5.29, N 15.68%.

2.3.3 Synthetic urine preparation and mimic synthetic urine of hyperuricemia patient

Synthetic urine was prepared as described in Sarigul, N. [58] All chemicals were dissolved in Ultrapure water, and the chemical composition of synthetic urine was listed in Table S4.1. The mimic synthetic urine of hyperuricemia patients was prepared by spiking urate into synthetic urine separately to obtain the final concentration of 1.50-6.50 nM. In comparison, synthetic urine samples spiked with 0.190-0.60 mM sodium oxalate and 2.45-5.50 mM trisodium citrate were measured to compare the sensitivity toward background ions in urine with urate.

2.4 Dual-dye probe construction

A probe contains 1:1:1 of eosin Y: Cu_2L: quinine sulfate by mol. The three components were mixed in 10 mM HEPES buffer pH 7.0 by adding 10 µL of 1 mM eosin Y, 5 µL of 2 mM Cu_2L, and 5 µL of 2 mM quinine sulfate. The final volume of probe solution was adjusted using 10 mM HEPES buffer pH 7.0 to obtain a 300 µL probe solution for the further fluorescence titration using a microplate reader.

2.5 Ratiometric fluorescence titration

All the ratiometric fluorescence titration of the dual-dye probe was reported in the fluorescence intensity ratio between signals from quinine sulfate and eosin Y: $I_{quinine\ sulfate}/I_{eosin\ Y}$ or I_{542}/I_{382} with the excitation wavelength at 330 nm. The fluorescence intensity was measured by using a microplate reader in a 96-black well plate.

2.5.1 Selectivity study

This selectivity of this probe to urate was studied over the other bio-relevant anions and urine-containing chemicals including terephthalate, malonate, fumarate, succinate, citrate, carbonate, urate, ascorbate, oxalate, phosphate, maleate, sodium sulfate, sodium chloride, magnesium phosphate, ammonium chloride, creatinine, sodium dihydrogen orthophosphate, and di-potassium hydrogen phosphate. The concentration of all compounds was set at 0.1 mM. The probe solution and other ions were pipetted into a 96-black well plate

2.5.2 Sensitivity study

There are three main anions that have positive results in this probe which are urate, oxalate, and citrate. However, sensitivity of this probe toward these three anions was different and was investigated by varying the concentration of anions from 0-100 µM.

2.5.3 Ratiometric fluorescence titration in synthetic urine

The varied volume of synthetic urine from 0-50 µL was pipetted into a 96-well plate containing 10 µL of 1 mM eosin Y, 5 µL of 2 mM Cu_2L, and 5 µL of 2 mM quinine sulfate. Then the volume was adjusted to 300 µL using 10 mM HEPES buffer pH 7.0.

2.5.4 Ratiometric fluorescence titration in synthetic urine, in patient mimics

The mimic synthetic urine of hyperuricemia patient and the oxalate and citrate spiked urine sample in 2.3.3) were diluted by 50-fold. The 100 μL of diluted solution was separately added into a well that contain 10 μL of 1 mM eosin Y, 5 μL of 2 mM Cu$_2$L, and 5 μL of 2 mM quinine. The final volume of each well was set to 300 μL by 10 mM HEPES buffer pH 7.0

3. Results and discussion

The dual-dye probe for urate-sensing was constructed from two commercial dyes with a synthetic dinuclear copper(II) complex, Cu$_2$L. The synthetic dinuclear copper(II) complex was synthesized from the macrocyclic ligand, L, and copper (II) nitrate. The ligand showed an H^1-NMR spectrum related to the previous report [57] (Figure S4.1), and the majority molecular mass is 411.32 m/z according to mass spectroscopy analysis (Figure S4.2).

The chemical composition and molecular mass of binuclear copper (II) complex, Cu$_2$L was characterized using a mass spectrometry technique and elemental analysis (CHN analysis). Mass spectrum provides a signal at 722.15 m/z, which is related to two copper (II) ions with one macrocyclic ligand and 3 stabilizing nitrate ions (Figure S4.3, Figure S4.4). The CHN analysis confirmed the percentage of carbon, hydrogen, and nitrogen as 36.69% of carbon, 5.29% of hydrogen, and 15.68% of nitrogen.

The characteristic fluorescence emissions of quinine sulfate and eosin Y are at 382 and 542 nm, respectively, which showing the blue and green fluorescence emissions. The addition of Cu$_2$L to eosin Y and quinine sulfate illustrated the difference in fluorescence response. Quinine sulfate did not exhibit any fluorescence response to Cu$_2$L, while the fluorescence of eosin Y was turned off in the presence of Cu$_2$L (Figure 4.1). It could be explained by the lacking of carboxylate group in

eosin Y. The carboxylate has preference to bind with Cu^{2+} in Cu_2L and causes the fluorescence quenching. Quenching of eosin Y could lead to an IDA system for detection of urate. Eosin Y would act as an indicator, Cu_2L is a host, and urate is the analyte. In the absence of the analyte, the fluorescence of the indicator was turned off upon the addition of Cu_2L. When the replacement of indicator, eosin Y, by urate was taken place, the turn-on fluorescence of eosin Y was detected in response to concentration of urate.

Interaction between the two dyes was investigated, and the results indicated that FRET was observed and could be utilized for enhancing the efficiency of urate detection. The characteristics of emission of quinine sulfate overlap with the characteristic absorbance of eosin Y (Figure 4.5), and the fluorescence titration between quinine sulfate and eosin Y confirmed the energy transfer from quinine sulfate to eosin Y (Figure S4.6). Thus, with the excitation wavelength of quinine sulfate at 330 nm (donor), the emission energy will transfer to eosin Y and acts as the excitation energy for eosin Y (acceptor).

In the combined concepts of the FRET between quinine sulfate and eosin Y and the IDA of eosin Y by urate on Cu2L host, the new urate-sensing approach in an aqueous solution was constructed. The fluorescence color changing from blue to green in combination with ratiometric fluorescence system was fabricated as a naked-eyes detection method as shown in Figure 4.1. The ratiometric fluorescence titration of this probe was reported in the fluorescence intensity ratio between the characteristic emission of eosin Y at 542 nm versus the characteristic emission of quinine sulfate at 382 nm: I542/I382.

The selectivity of the new approach dual-dye sensing system was studied over the bio-relevant anions and the other chemical composition that can be found in urine (Figure 4.3). This probe demonstrated a fluorescence response to three main anions urate, oxalate, and citrate. The selectivity of the probe depends on the

binding abilities of analyze to dinuclear copper (II) complex, Cu_2L, related to the previous publications [1, 36]. This complex was published as an oxalate sensing [36] by the replacement of eosin Y or fluorescein dyes by oxalate ions, and it provided a high selectivity to oxalate ions but there was no selectivity study toward urate and citrate. While in 2020, *Hontz, D. et. al.* [1] reported a stronger fluorescence response of urate ions than oxalate ions with the same complex, and it demonstrated a weaker response to citrate than oxalate.
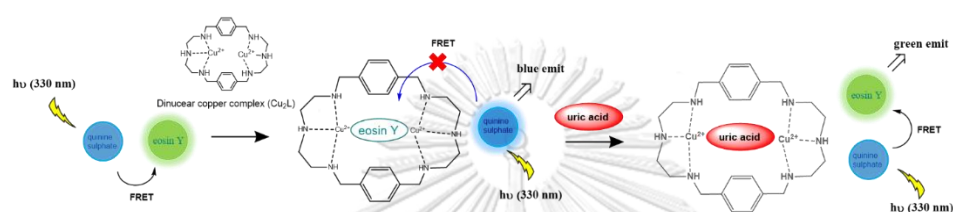
Figure 4.1 Strategy scheme of the dual-dye probe for urate sensing.
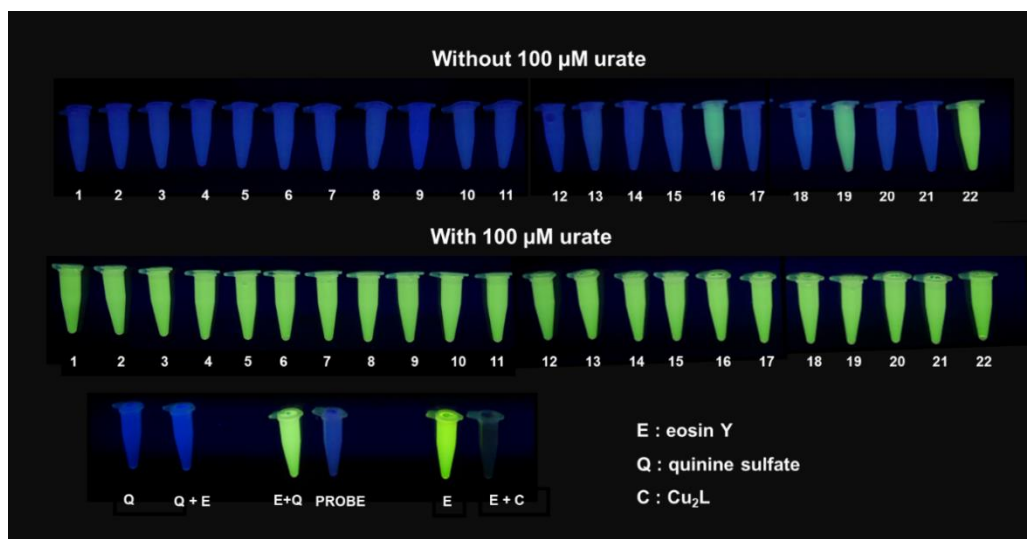
Figure 4.2. The image of fluorescence signals from the solution of different ions with and without urate ions, 1 -22: 1. potassium sulfate, 2. sodium chloride, 3. magnesium sulfate, 4. urea, 5. ammonium chloride, 6. sodium dihydrogen orthophosphate, 7. calcium chloride, 8. sodium sulfate, 9. creatinine, 10. di-potassium hydrogen phosphate, 11. no anions, 12. terephthalate, 13. malonate, 14. fumarate, 15. Succinate, 16. citrate, 17. carbonate, 18. ascorbate, 19. oxalate, 20. phosphate, 21. maleate, and 22. urate, respectively.
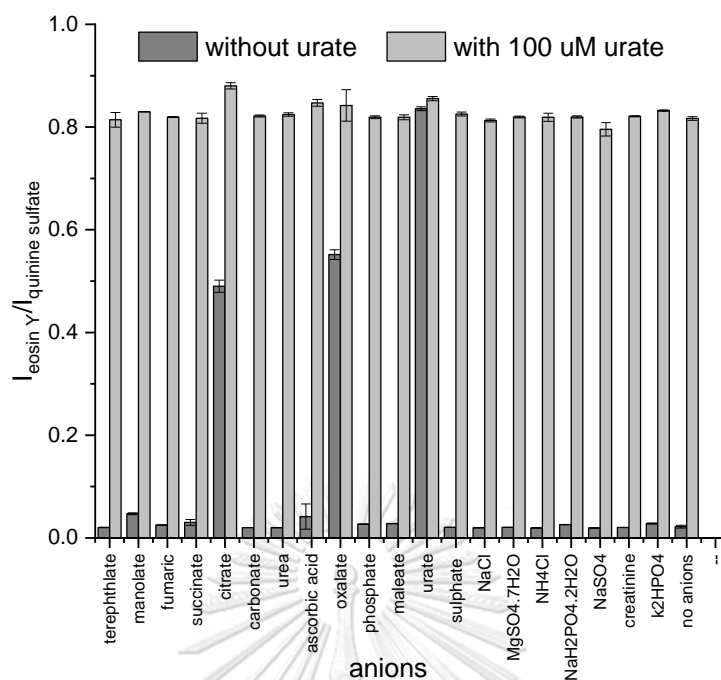
Figure 4.3. The selectivity study of the proposed urate sensor with and without urate, the concentration of all ions is 100 µM.

When comparing the sensitivity of the probe toward the three ions under the same condition, urate showed highest sensitivity, Figure 4.4. illustrates the ratiometric fluorescence titrations of the dual-dye probe and urate. Upon the addition of urate, the fluorescence recovery of eosin Y was observed. The detection limit, LOD, of this probe was calculated by 3SD/SL, where SD is the standard deviation of blank and SL is the slope of the linear plot. LOD's for the detection of urate, oxalate, and citrate were equal to 0.0699, 0.3790, and 1.0472 µmol L^{-1}, respectively (Figure S4.1) with the linear range from 0-30, 0-50, and 0-50 µM, respectively. Sensitivity toward urate, oxalate, and citrate ions of these probe was high enough for detection the abnormal level of these three metabolites because these LOD's are significantly lower than the normal level of these ions found in human urine [43, 59].
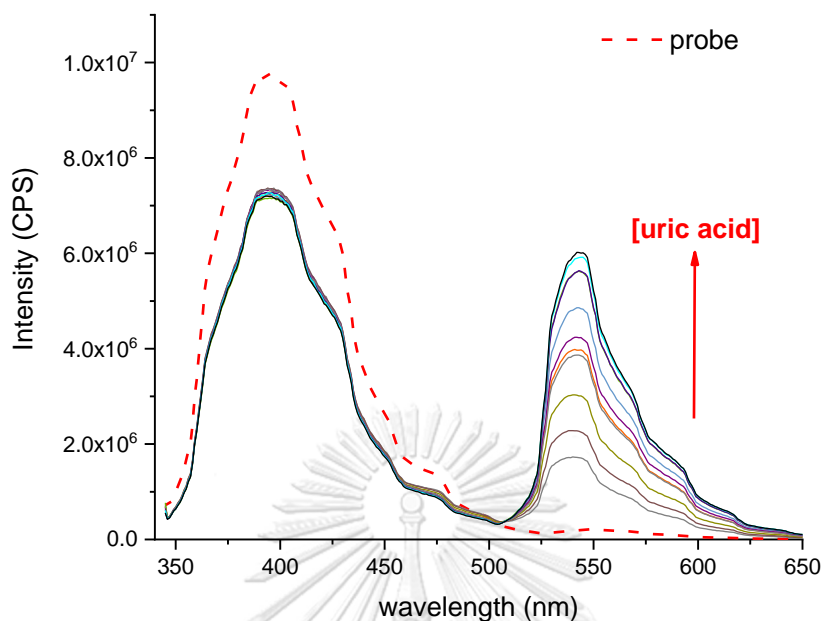
Figure 4.4 The fluorescence spectra of the dual-dye probe in the addition of urate.

To develop this probe for detection of abnormal level urate in the urine samples, the detection of additional urate in synthetic urine, with inclusion of urate, citrate and oxalate ions in the background has been studied. At first, the fluorescence titration of this probe with the synthetic urine was performed to find the optimal range of urine concentration that the background urate, oxalate and citrate could not overflow the signals from the abnormal level of the analytes. With the increase in the synthetic urine volume, I542/I382 value was recovered back to the initial value (1.0) and remained at about 1.0 at the high volume of synthetic urine (Figure 4.5). Therefore, the volume of synthetic urine in further study was set in the middle of the linear slope. It was found that under optimized dilution factor, this probe can clearly distinguish the samples with normal urate concentration (0.7-2.3 mM) [48, 49] and samples with higher level of urate up to 6.50 mM (Figure 4.6a). However, this probe was not sensitive enough to distinguish oxalate and citrate ion of slightly higher concentration than the background ions (Table S1) in the synthetic urine (Figure 4.6b,c).This new ratiometric dual-dye probe was successfully developed

for urate detection in synthetic urine. Under optimized dilution, the probe is sensitive enough to quantify the abnormally high level of urate specifically.
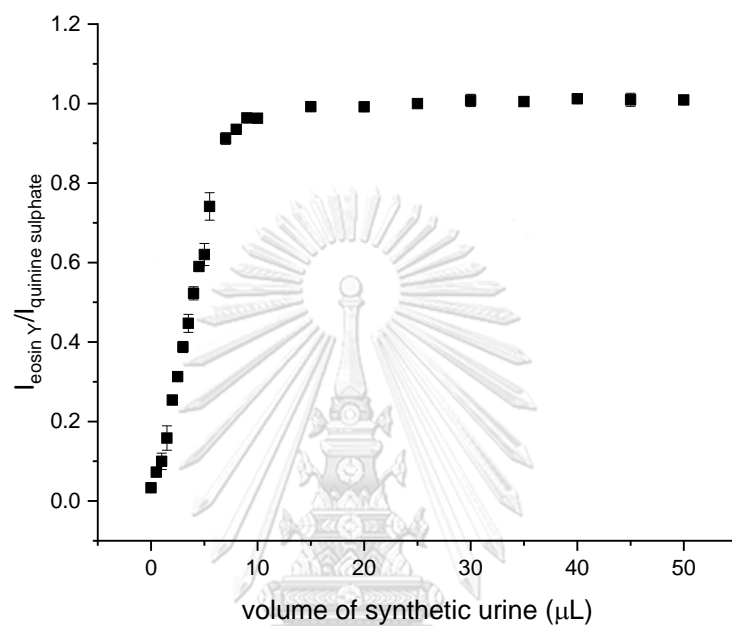
Figure 4.5 The ratiometric fluorescence response curve upon the increase in the quantity of synthetic urine.
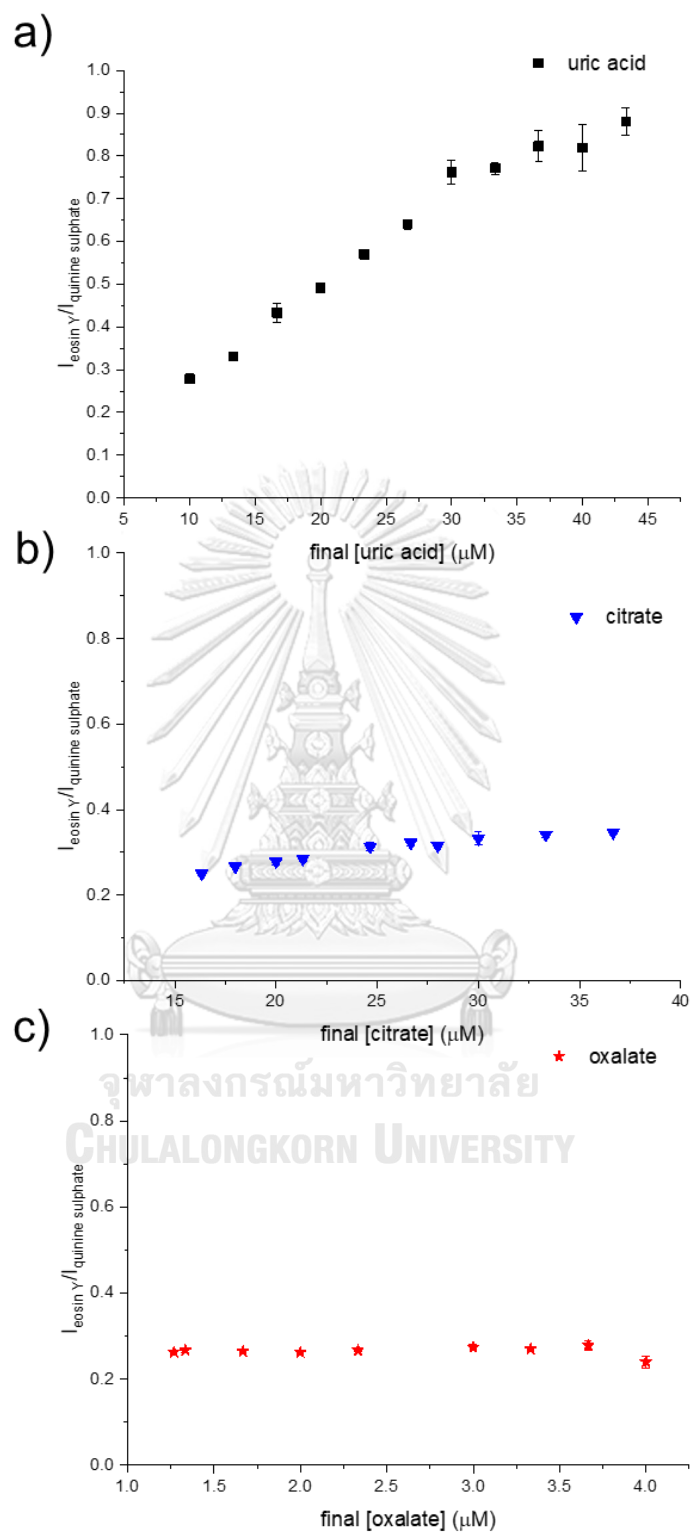
Figure 4.6 The ratiometric fluorescence response curves of the synthetic urine spiked with (a) urate, (b) citrate ion, and (c) oxalate ion.

4. Conclusion

In summary, we have reported the new urate detection system which is based on the ratiometric fluorescence method called the dual-dye probe. This probe is rapid and sensitive to urate in synthetic urine. This dual-dye probe shows the good selectivity toward the other bio-relevant ions and the urine ions of concern including potassium sulfate, sodium chloride, magnesium sulfate, urea, ammonium chloride, sodium dihydrogen orthophosphate, calcium chloride, sodium sulfate, creatinine, di-potassium hydrogen phosphate, terephthalate, malonate, fumarate, succinate, carbonate, ascorbate, phosphate, and maleate. This probe has also showed sensitivity in the detection of oxalate and citrate ions in aqueous solution with background of their common ions.

This dual-dye probe demonstrated the ratiometric fluorescence sensor made up of two commercial dyes that have a high photostability and high quantum yield. This probe construction leads to the stable naked-eyed detection under the UV lamp and avoids the color of the sample interference. With further development, this probe could be used for the onsite prescreening of urine from patients with the risk of hyperuricemia enabling early prevention of more severe illness.

5. Acknowledgements

Supplementary information I

Table S4.1 The synthetic urine composition.

chemicals	concentration (mM)
sodium oxalate	0.190
sodium chloride	30.053
magnesium sulfate	4.389
urea	249.750
ammoniamchloride	23.667
sodium dihydrogen orthophosphate	18.667
calcium chloride	1.663
tri-sodium citrate	2.450
sodium sulfate	11.965
uric acid	1.487
creatinine	7.791
di-potassium hydrogen phosphate	4.667
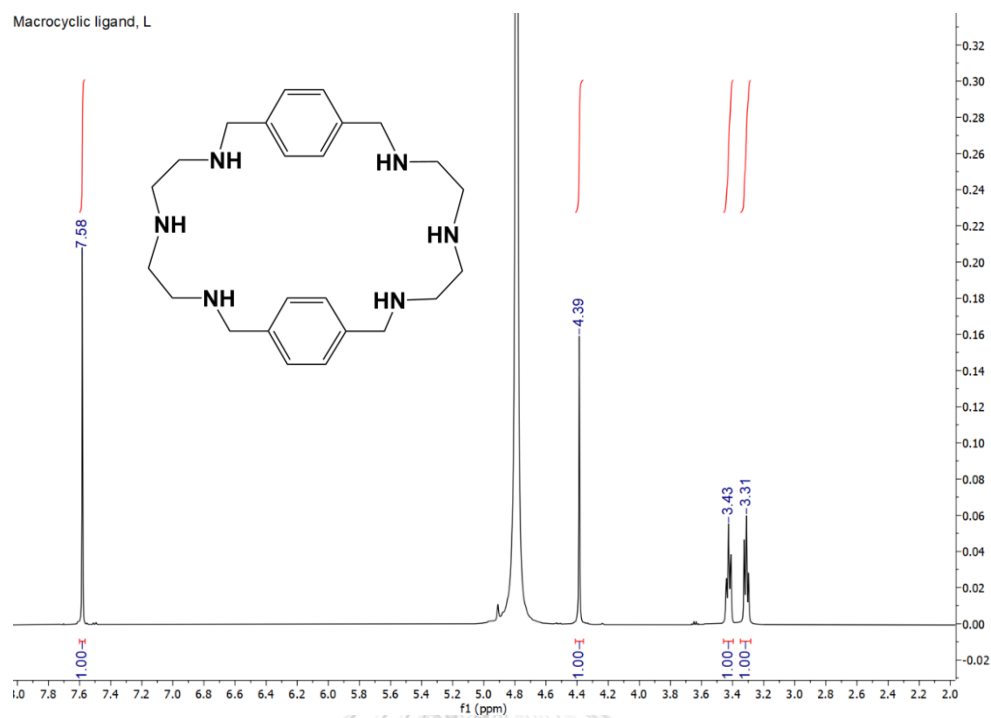
Figure S4.1 H^1-NMR of macrocyclic ligand, L.
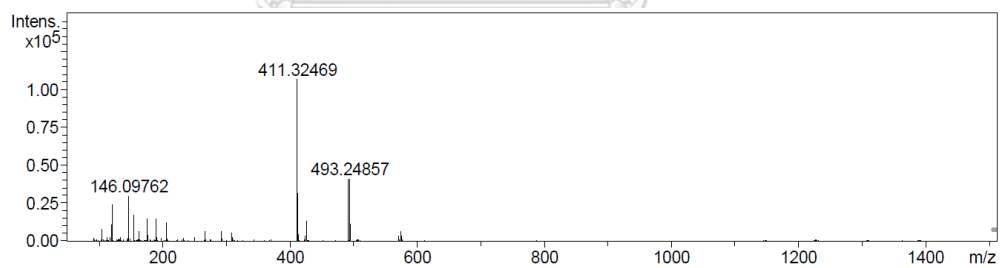
Figure S4.2 Mass spectrum of macrocyclic ligand, L.

Chemical Formula: $C_{24}H_{38}Cu_2N_9O_9{}^+$
Exact Mass: 722
Molecular Weight: 724
m/z: 722 (100.0%), 724 (89.1%), 723 (26.0%), 725 (23.1%), 726 (19.9%), 727 (5.2%), 723 (3.3%), 724 (3.2%), 726 (2.4%), 724 (1.8%), 726 (1.6%), 725 (1.6%), 725 (1.3%)
Elemental Analysis: C, 39.83; H, 5.29; Cu, 17.56; N, 17.42; O, 19.90

Chemical Formula: $C_{24}H_{38}Cu_2N_{10}O_{12}$
Exact Mass: 784
Molecular Weight: 786
m/z: 784 (100.0%), 786 (89.1%), 785 (26.0%), 787 (23.1%), 788 (19.9%), 789 (5.2%), 785 (3.7%), 786 (3.2%), 786 (2.5%), 788 (2.4%), 788 (2.2%), 787 (1.6%), 787 (1.6%)
Elemental Analysis: C, 36.69; H, 4.88; Cu, 16.18; N, 17.83; O, 24.43

Figure S4.3 Copper (II) complex, Cu_2L structure, and ChemDraw calculation for each possible structure of Cu_2L.
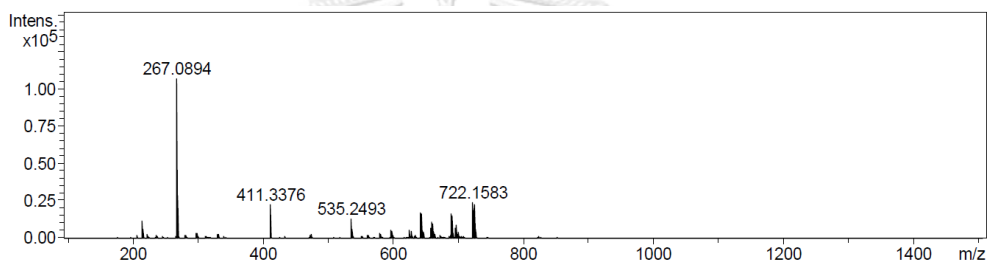
Figure S4.4 Mass spectrum of copper (II) complex, Cu_2L.
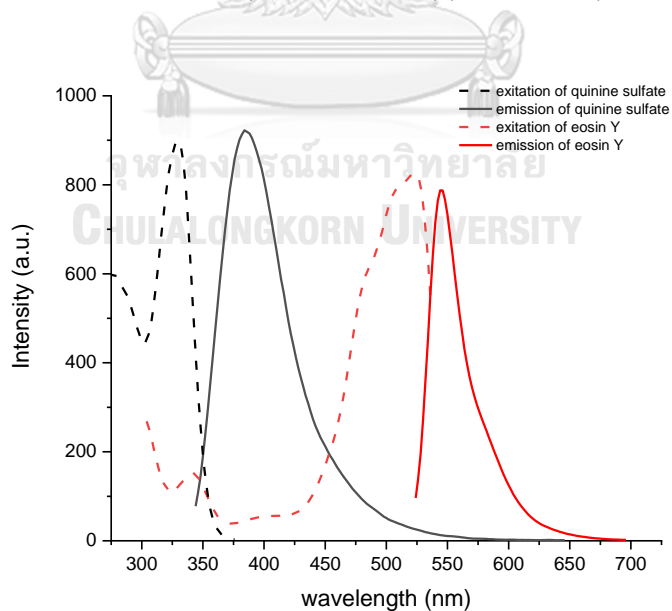
Figure S4.5 PL spectra of quinine sulfate and eosin Y.
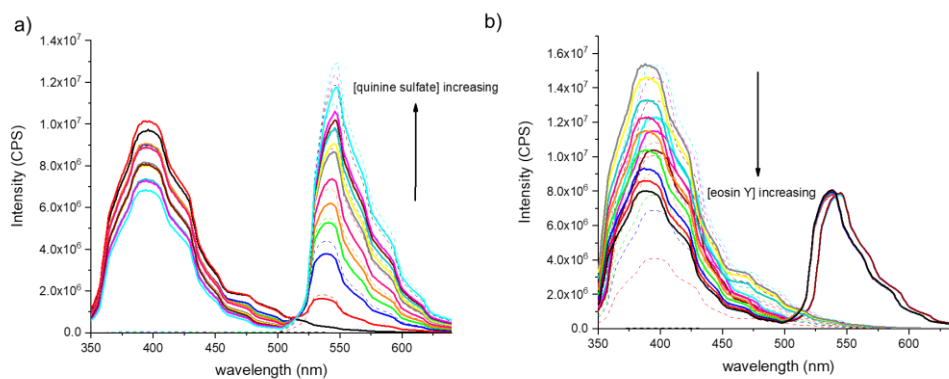
Figure S4.6 The fluorescence titration spectra of a) a fixed amount of quinine sulfate in varying the amount of eosin Y and b) a fixed amount of eosin Y in varying the amount of quinine sulfate (dash lines are the reference emission spectra of dyes at each concentration).
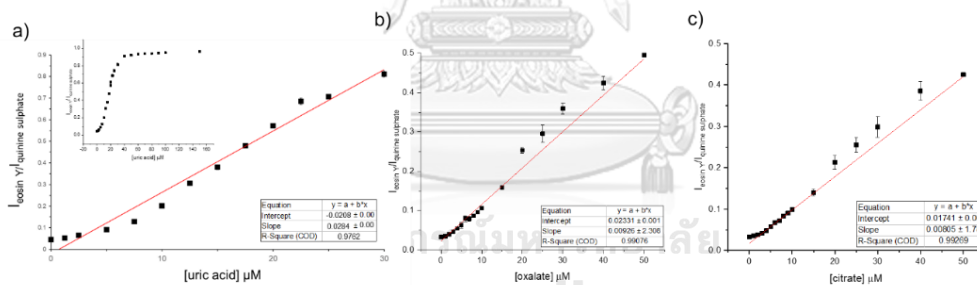
Figure S4.7 The ratiometric fluorescence response curve of urate a), oxalate ion b), and citrate ion c).

CHAPTER V

Fluorescent responses of CdSe and Si QDs toward Copper (II) ion and the mixed-QDs probe for Copper (II) ion sensing

Authors: Nattakarn Phromsiri[a], Sakiru L. Abiodun[b], Chonnavee Manipuntee[a], Pannee Leeladee[a], Andrew B. Greytak[b], Numpon Insin[*a].

[a] Department of Chemistry, Faculty of Science, Chulalongkorn University, Thailand

[b] Department of Chemistry and Biochemistry, University of South Carolina, Columbia, SC 29208, USA

1. Abstract

Although copper(II) ion is essential for the human body, but an excess of Cu^{2+} causes damage to the human cell and is implicated in many diseases. Cu^{2+} is also counted among heavy metal pollutants in the environment, especially in water. Thus, a new approach towards quantifying Cu^{2+} ion is appealing. Here, we reported a new ratiometric mixed-QDs probe for Cu^{2+} detection in an aqueous solution with the combined concept of ratiometric and fluorescence resonance energy transfer. This probe consists of blue Si QDs (donor) and yellow CdSe QDs (acceptor). The energy transfer from Si QDs and CdSe QDs was confirmed by the time-resolved fluorescence. The changes in the ratiometric fluorescence response of the mixed-QDs probe upon exposure to Cu^{2+} were studied using fluorospectrometry, while the mechanism of the Cu^{2+} quenching to the probe was studied using an X-ray photoelectron spectrometer. This approach is a simple, fast, sensitive and accurate method for Cu^{2+} sensing which has a low detection limit (3.89 nmol L-1). Moreover, this methos has a high selectivity to Cu^{2+} versus other biological relevant cations and

cations of high environmental impacts. Furthermore, this new mixed-QDs probe could be used as a naked-eye detection of Cu^{2+} for water samples and biological specimens with further development.

Highlight : quantum dots, CdSe QDs, Si QDs, copper (II) ions, sensor, ratiometric fluorescence

2. Introduction

Colloidal semiconductor nanocrystals (also called quantum dots,-QDs) have attracted much attention due to their unique optical and electronic properties. These properties include their tunable fluorescence and absorption spectra which can be attributed to quantum confinement. These properties have led to QDs being widely investigated in applications such as drug delivery [7, 60], fluorescent markers for bioimaging [10, 42, 61], optical-electronic devices [62-63], immunoassays [25, 64-65], and fluorescence-based sensing [8, 11, 25, 33, 45, 59, 61, 66-78].

In recent years, QD-based fluorescence sensing has been targeted for the detection and measurement of biochemical conditions, pharmacological substances, and environmental pollutants with potential advantages in economy [77], sensitivity, and simplicity. The general schemes for fluorescent detection using QDs include 'turn-on' mechanisms, where the fluorescence intensity is enhanced by the addition of analytes, and 'turn-off' mechanisms, in which quenching of fluorophores occurs in response to an analyte via direct quenching, photoinduced electron transfer (PET), and/or fluorescence resonance energy transfer (FRET) processes. Among QD compositions, there are many types that have been used for fluorescence sensing applications to date, notably including : CdSe [8, 73], CdSe/ZnS [74, 78], CdTe [33, 70, 75, 79], CdTe/ZnS [33], metal modified CdS [45], ZnSe/ZnS [76], $CuInS_2$ [52], Si QDs [10-11, 25, 61, 68].

CdSe QDs are widely used as fluorescence probes due to their high photostability and tunability across the visible spectrum. CdSe QDs can be prepared mainly from two solvent systems: high boiling point organic solvents with coordinating surfactants, and aqueous-based systems. CdSe QDs that are prepared at high-temperature organic solvents usually exhibit superior fluorescent properties, but often times a surface modification process is required to allow the QDs to be dispersible in water for further uses. In contrast, CdSe QDs prepared from water-based systems are readily water-dispersible when hydrophilic capping agents are used during the synthesis and can be natively attached to protect the QDs surface [53]. Some common stabilizing agents are 3-mercaptopropionic acid (MPA), L-glutathione (GSH), thioglycolic acid (TGA), and *N*-acetyl-L-cysteine (NAC). There have been many reports on the CdSe QDs that are prepared using water-based systems as it is relatively convenient in handling, but low photostability and sensitivity to variations in pH and ionic strength are of some concerns.

In a similar vein, Si QDs have also been reported to be used in fluorescence sensing for the detection of various analyzes, such as explosive molecules [54], organic compounds [80], alkaline phosphate [11], ethyl carbonate [25], glucose [81], and dyes [68] due to their high photostability, biocompatibility, low cytotoxicity, and surface paint-ability. Moreover, the preparation method of aqueous-based Si QDs is simple, low-cost, and non-toxic. To fabricate Si QDs-based fluorescence sensors, other molecules that are photoactive are usually required because Si QDs themselves have very high photostability and hardly respond to the analytes. There are a few reports using the organic molecules (in complementary to Si QDs) with aza crown [61] and azo group [68] to complete the electron transfer process, but to the best of our knowledge, there is no report on using Si QDs with other types of quantum dots. Furthermore, the emission energy of Si QDs is in the blue emission range which enables them to serve as a good energy donor for other visible-emitting fluorophores in the photoinduced electron transfer (PET) and fluorescence resonance energy transfer (FRET) processes.

In this work, we made use of the high photostability of blue-emitting Si QDs to design a new fluorescent probe.

Copper, while required as a nutrient, is identified as one of the toxic metals in water that can negatively affect animals, plants, and humans. An excess amount of copper in the human body can cause the risk of many diseases, such as Alzheimer's disease, prion disease, Wilson's disease and Parkinson's disease [63, 77, 82-83]. The traditional methods for the detection of copper include the use of inductively coupled plasma-mass spectroscopy (ICP-MS), inductively coupled plasma - optical emission spectrometry (ICP-OES), and atomic absorption spectroscopy (AAS). However, these techniques are expensive, time-consuming, and required skillful users. Therefore, the development of copper detection probes has received a big interest to be a simple, sensitive, fast, accurate, and low detection limit sensing probe. In recent years, the quantum dots-based fluorescence sensors has been widely studied for Cu^{2+} detection due to their high photostability [33, 45, 73, 75-78]. The detection of Cu^{2+} by fluorometric detection of QDs has been reported. Unfortunately, other metals ions, such as Hg^{2+} and Ag^+ also lead to the quenching of CdSe/ZnS QDs in the Cu^{2+} sensing system by fluorometric detection of CdSe/ZnS [78]. This makes accurate determination of Cu^{2+} in any system more difficult. In addition, Mn^{2+} also "turn on" the fluorescence of Si QDs similar to Cu^{2+} thus, these Si QDs were used as a dual detection probe [77].

On the another hand, ratiometric fluorescence probes have been reported and showed significant improvement from the intensity-based systems for many reasons [84]. The ratiometric system, in which the ratio of fluorescence measured at two different emission and/or excitation wavelengths composes the signal, is self-correcting, so that interferences from the probe concentration, media, and instrumental factors, such as excitation power are eliminated. As a result, a separate internal standard is not required for the dual photoluminescence system, and complicated and high interference specimens, such as biological samples, can be

readily analyzed. Also, naked-eye detection is promising for the ratiometric systems as the probes can give obvious changes of perceived emission color on exposure to the targeted condition or analyte. A ratiometric fluorescence probe for copper (II) ion detection has been reported by using CdTe QDs and metal-organic frameworks (MOFs) [70]. This ratiometric detection of CdSe/MOFs can overcome the effects of many interferences including Mn^{2+} and Ag^+, but the fluorescent signals can also be quenched by Hg^{2+} ions. Therefore, emitter combinations are required for ratiometric probes that have lower undesired quenching from interfering ions, and high photostability.

In this work, we report a new fluorescent probe consisting of mixed-QDs: Si QDs and CdSe QDs for sensitive and selective copper(II) ion detection in an aqueous solution. X-ray photoelectron spectroscopy technique (XPS) was used to understand the quenching mechanism of the CdSe QDs which plays the dominant role in the mixed-QDs probe to detect Cu^{2+}. Blue-emitting Si QDs were selected as the FRET donor and yellow-emitting CdSe QDs as FRET acceptor. Naked eye detection of the analyte was done under a UV lamp by observing the change in emission colors. Our result opens the door to the application of mixed Si QDs/CdSe QDs for naked eye Cu^{2+} detection in various samples.

3. Experimental

3.1 Si QDs synthesis

The synthesis of Si QDs was based on a reported method [10] with some modifications. Briefly, Si QDs were synthesized by the hydrothermal method. 1 g of tri-sodium citrate was dissolved in 21.5 mL Milli Q water and was bubbled in nitrogen gas for 15 min. Then 5.36 mL APTES was added into the solution. Finally, the mixture was transferred into a 100 mL Teflon-lined stainless-steel autoclave and heated at a

constant temperature of 200 °C for 4 h. Si QDs were purified by washing and centrifugation in ethanol several times. Si QDs were redispersed in Milli Q water and kept in the dark at 4 °C for further use.

3.2 CdSe QDs synthesis

The synthesis of CdSe QDs was based on a reported method [8]. Typically, 0.80 mL of 0.20 M $CdCl_2$ solution was diluted in 50 mL of Milli Q water in a flask with a vigorous stir. Then, 34.6 µL of MPA was added into the solution followed by sufficient 1.0 M NaOH to adjust the pH to 9.0. Then, 0.80 mL of 0.02 M Na_2SeO_3 was injected into the flask. After the solution was refluxed at 100 °C for 5 min, 3.67 mL of $N_2H_4 \cdot H_2O$ was loaded into the solution. The yellow CdSe QDs solution was obtained after 12 h of refluxing at 100 °C under air. The synthesized QDs were purified by washing with ethanol and centrifugation. Lastly, CdSe QDs were redispersed in Milli Q water and kept in the dark at 4 °C for further use.

3.3 Mixed-QDs probe construction

300 µL of Si QDs (absorption value = 0.2, λ_{abs} = 350 nm) and 60 µL of CdSe QDs (absorption value = 0.15, λ_{abs} = 350 nm) were dissolved in 10 mM pH 7.0 HEPES buffer under the vigorous stirring. The final volume was adjusted to 3 mL to obtain the mixed-QDs probe solution for further study.

3.4 Characterization of quantum dots

The optical properties of QDs were characterized by UV-VIS and fluorescence spectrometries. The sizes and planes of the dots were measured using a field emission transmission electron microscope (FETEM). The functional group of the dots was obtained by a fourier tansform infrared (FTIR) technique.

3.5 Fluorescence titration

Quenching of Si and CdSe QDs by copper (II) ion was studied by fluorescence spectroscopy. 300 μL of Si QDs (in milli-Q water, absorption value = 0.2, λ_{abs} = 350 nm) and 60 μL of CdSe QDs (in milli-Q water, absorption value = 0.15, λ_{abs} = 350 nm) were transferred to a vial. Then, the total volume was brought to 3 mL by the addition of 10 mM pH 7.0 HEPES buffer Then, a slight amount of Cu^{2+} ions from 10 mM $Cu(NO_3)_2$ was injected into the solution to give the final concentration of free copper ion as 0-16 μM.

The detection of Cu^{2+} by the mixed-QDs probe was studied by the fluorescence titration between mixed QDs-probe and Cu^{2+} ion solution at various concentrations from 0 nM – 200 nM.

3.5.1 Fluorescence lifetime analysis

The fluorescence lifetime analyses were conducted at room temperature using a Horiba DeltaFlex spectrophotometer with a 375 nm pulsed laser diode excitation. Decay lifetimes were collected through a monochromator centered at either 485 nm for Si QDs or 575 nm for CdSe QDs with an emission bandwidth of 6 nm and a time range of 100 ns.

3.5.2 Selectivity study

In order to test the selectivity of the sensor for Cu^{2+}, the response to various metal ions including Co^{2+}, Fe^{3+}, Zn^{2+}, Al^{3+}, Mg^{2+}, Cr^{3+}, Ba^{2+}, Li^+, Ca^{2+}, Sr^{2+}, Ag^+, Na^+, Ni^{2+}, K^+, Cd^{2+}, Pb^{2+}, Mn^{2+}, and Hg^{2+}, was detected using the procedure below.

Selectivities of Si QDs, CdSe QDs, and mixed-QDs probe were studied. Separately, Si QDs, CdSe QDs, and the mixed-QDs probe with and without Cu^{2+} were added in a 96 well plate. Then, 6 μL 50 μM $Cu(NO_3)_2$ solution, or one of the other

metals was added into each well, and the final volume of each well was adjusted to 300 μL by 10 mM HEPES buffer pH 7.0. The concentration of all metals was set at 1 μM. The plate was shaken automatically on the microplate reader for 15 min at 100 rpm before the fluorescence measurement.

4. Result and discussion

4.1 Characterization of the synthesized quantum dots

Si QDs were synthesized based on the previous report [10-11] with modification in the heating system from using a microwave oven to a hydrothermal method under a Teflon-lined stainless-steel autoclave at 200 °C. After 4 h, Si QDs were purified by ethanol. APTES was used as a silicon source for Si QDs with citrate as a stabilizing ligand. Blue-emitting Si QDs were obtained after the reaction and purification process. The UV-VIS absorption band and fluorescent spectra of Si QDs was illustrated in Figure 5.1. The characteristic first absorption peak of Si QDs at around 347 nm and the symmetric emission band at 430 nm corresponding to the blue emission color (Figure S5.1b) were obtained. In FTIR spectra, several distinct transmittance peaks appear in the range of 1000–3500 cm^{-1}. Typically, the broad absorption peak at $\sim$ 3120-3400 cm^{-1} is assigned to O-H stretching vibration. The absorption peak at $\sim$ 1580-1650 cm^{-1} can be attributed to C=O stretching vibration which indicates the production of –COOH and the absorbance at $\sim$1390-1400 cm^{-1} corresponded to C-O stretching vibration. Most importantly, the strong absorption peak at $\sim$1100 cm^{-1} is ascribed to the Si-O bonding vibration stretching, which proved that Si QDs were successfully synthesized. Moreover, FETEM and SAED images in Figure 5.4c demonstrated the size, morphology, and crystal lattice of quantum dots. The average diameter of Si QDs is 2.50 ± 0.30 nm with spherical particles and well dispersion. Additionally, the SAED image of Si QDs demonstrates the crystal lattice

related to (111), (220), and (211) lattice planes with the d spacing equal to 3.14, 1.01, and 1.59 Å, respectively. The elemental analysis of these Si QDs by using energy-dispersive X-ray spectroscopy (EDS) proves that Si QDs contain Si, C, O, and N. X-ray photoelectron spectroscopy (XPS) was used to study the surface composition of Si QDs. Full-scan XPS spectra of Si QDs, showed five distinct peaks at 1070 eV, 532 eV, 399 eV, 285 eV, and 102 eV which are related to Na 1s, O 1s, N 1s, C 1s, and Si 2p, respectively, as shown in Figure 5.2a.

CdSe QDs were synthesized using hydrothermal method under the air atmosphere at 100 $^\circ$C for 12 h in an aqueous solution without any shell coating based on the previous report [8]. Hydrazine was used as a reducing agent to reduce Se^{4+} to Se^{2-} without an oxygen-free atmosphere, and MPA was used as a stabilizing ligand to stabilize CdSe in an aqueous solution. A yellow-emitting CdSe QDs was obtained as shown in Figure 5.4. The obtained CdSe QDs were characterized by UV-VIS, fluorescence spectroscopy, FETEM, FTIR, and XPS measurements. Figure 5.1a shows the optical properties of CdSe QDs with the first absorption at around 549 nm and emission at 573 nm with a symmetric peak. The FETEM images of CdSe QDs showed well dispersion of spherical particles with an average diameter of 3.82 ± 0.77 nm. The SAED image illustrated the d-spacing of CdSe of 3.50, 2.14, 1.83 Å corresponding to (111), (220), and (311) lattice planes (Figure 5.1d.) The elemental analysis of these CdSe QDs using EDS represents the compositions of C, O, S, Se, and Cd. The FTIR spectra of CdSe QDs showed the transmittance peaks at 〜 3120-3450, 〜 1586, 〜 1400 cm^{-1}, which were described to O-H stretching, C=O stretching vibration, and C-O stretching vibration, respectively. FTIR spectra demonstrated that CdSe QDs and Si QDs have many hydroxyl groups, Figure 5.1b. Full-scan XPS spectra of CdSe QDs (Figure 5.2b) showed six distinct peaks at 1072 eV, 532 eV, 405 eV, 295 eV, 168 eV and 54 eV which were related to Na 1s, O 1s, Cd 3d, C 1s, S 2p and Se 3d, respectively. It is confirming the existence of Cd, Se, S in CdSe QDs.
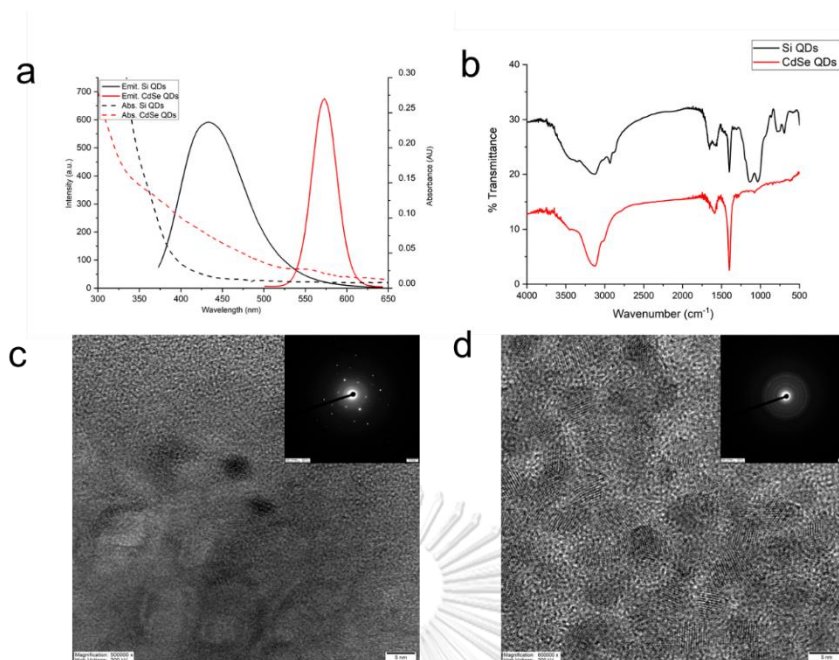
Figure 5.1 Absorbance and PL spectra (a), FTIR spectra (b), and FETEM images of Si QDs (c) and CdSe QDs (d).
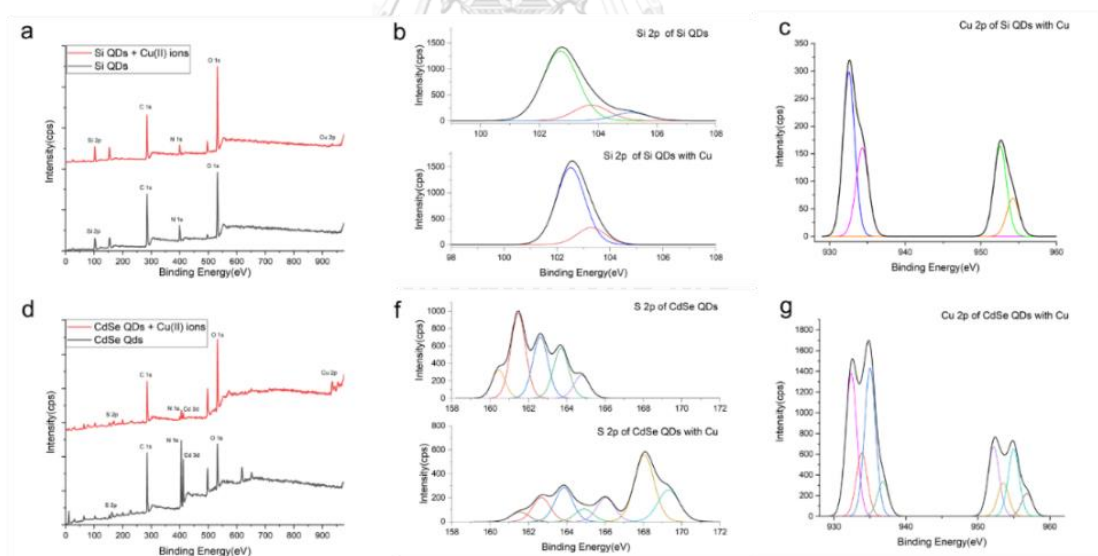
Figure 5.2 Full scan XPS spectra of Si QDs (a) and CdSe QD (d) and high-resolution XPS spectra of Si QDs at Si 2p (b), Cu 2p (c), of CdSe QDs at S 2p (f), and Cu 2p (g).

4.2 Quenching study: Detection of copper (II) ion
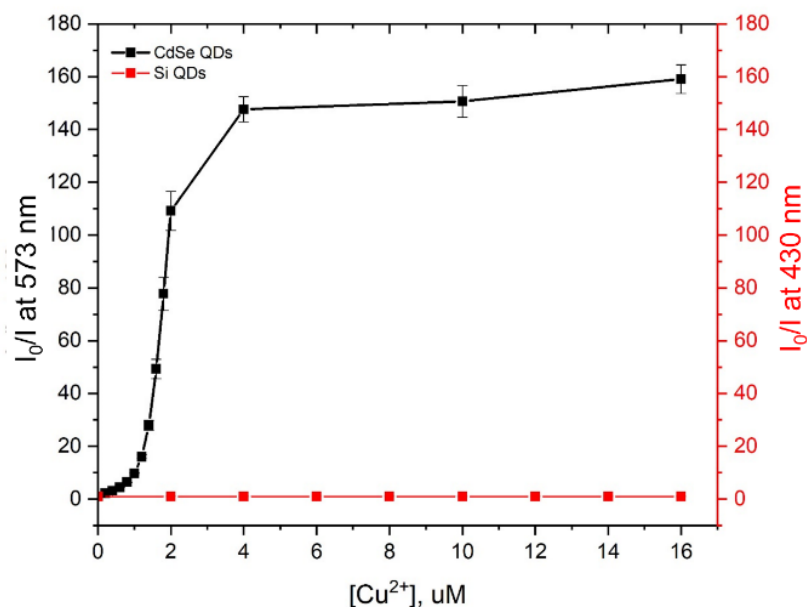
Figure 5.3 The stern-Volmer plot of CdSe QDs compared to Si QDs upon copper (II) quenching.

The quenching of Si QDs and CdSe QDs by Cu^{2+} was studied using fluorescence spectroscopy. Aliquots of CdSe QDs and Si QDs were dissolved in HEPES buffer 10 mM at pH = 7 and titrated with a small volume of copper (II) nitrate solution from 0.20 – 16.0 µM in the separate fluorescent cuvette. PL spectra of the titration provides information on the fluorescence intensity at the characteristic emission of CdSe QDs as shown in Figure S5.2. The fluorescent signals were gradually decreased upon the addition of copper (II) ion, while fluorescence intensity of Si QDs did not experience any significant change in the intensity at the same concentration of added Cu^{2+}.

The fluorescence quenching of CdSe QDs can be described by the Stern-Volmer equation as follow: $I_0/I = 1+K_{sv}[Q]$, where I_0 and I are the fluorescence intensity in the absence and presence of quencher, [Q] is quencher concentration and K_{SV} is a Stern-Volmer constant.

The Stern-Volmer plot comparing the effect of Cu^{2+} ions to QDs in the concentration range from 0.2- 16 µM in Figure 5.3, indicating the clearly quenched CdSe QDs in the presence of free copper (II) ions. Commonly, the quenching of fluorophore takes place through the static and/or dynamic interaction between fluorophore and quencher [76]. The deviations were observed at the higher concentration of Cu^{2+} which is probably related to the simultaneous existence of both statistic and dynamic quenching [79].

The surface information of water dispersible CdSe QDs and Si QDs was investigated by X-ray photoelectron spectroscopy (XPS) analysis. XPS survey spectra of CdSe QDs and Si QDs were compared in the presence and absence of Cu^{2+} ions as shown in Figure 5.2**Error! Reference source not found.**a,d. The peak of Cu 2p was obviously observed at 932 eV for CdSe QDs, indicating the significant deposition of copper on the surface of CdSe QDs. On the other hand, XPS spectra of Si QDs exhibited only a tiny peak of Cu 2p. The observation of the different in copper composition on the surface can imply that copper (II) ions have higher tendency to deposit onto CdSe QDs surface rather than Si QDs. This observation can be related to the possible mechanisms of the fluorescent quenching of CdSe QDs by Cu^{2+} as have been discussed previously as 1) the reduction of Cu (II) ion on the surface of CdSe QDs [18, 75, 85], 2) Cation exchange on the surface of CdSe QDs [74], and 3) the K_{sp} of CuS, CuSe lower than CdSe [70, 75].

Detailed investigation on XPS analysis was done to better understand this phenomenon. The XPS spectra of CdSe in the presence of Cu^{2+} ions demonstrated that Cd (II) ions remained on the surface, but they were disturbed by Cu^{2+} as the intensity of the main Cd peak decreased with slight redshift on the binding energy (Figure S5.3), while in Si QDs, only small tail loss (Figure 5.2b) It can be implied that Cu^{2+} bound more effectively on the surface of CdSe QDs than Si QDs. Furthermore, at Cu 2p of high-resolution XPS spectra of CdSe (Figure 5.2g), various species of Cu including Cu^{0}, Cu^{+}, and Cu^{2+} were detected, but they were not observed in Si QDs.

This observation can be related to the partial reduction of Cu^{2+} on the surface of CdSe QDs into Cu^+ and Cu^0, and Cd^{2+} on the surface can then be replaced by Cu ions that were reduced. Moreover, that high-resolution XPS at S 2p (Figure 5.2f) demonstrated the oxidation of S^{2-} and -SH on the surface of QDs to sulfate and thiosulphate at 168.0 and 169.3 eV. Another reason for the high ability of Cu^{2+} in quenching of CdSe QDs could be the formation of CuS on the surface of CdSe QDs leading to non-radiative process for the exciton as the K_{sp} of CuS (6.0×10^{-37}) [70] is lower than K_{sp} of CdSe (6.3×10^{-36}) [74]. In comparison to the XPS analysis of Si QDs, the high-resolution XPS of Si QDs at Cu 2p illustrated the existence of Cu on the surface of QDs, but with lower intensity than on CdSe QDs. The reason for small Cu deposition could be that the functional group on Si QDs was mainly carbonyl group from sodium citrate capping agent, which has lower binding affinity with Cu^{2+}. Upon the detailed investigation in combination with the fluorescence titration and Stern-Volmer's plot, it can be inferred that Cu^{2+} mainly quench CdSe QDs but not Si QDs. The different effects of Cu^{2+} on Si QDs and CdSe QDs lead us to the idea of a naked eyes Cu^{2+} sensing probe called a mixed QDs probe.

4.3 Copper detection method by mixed QDs probe

4.4
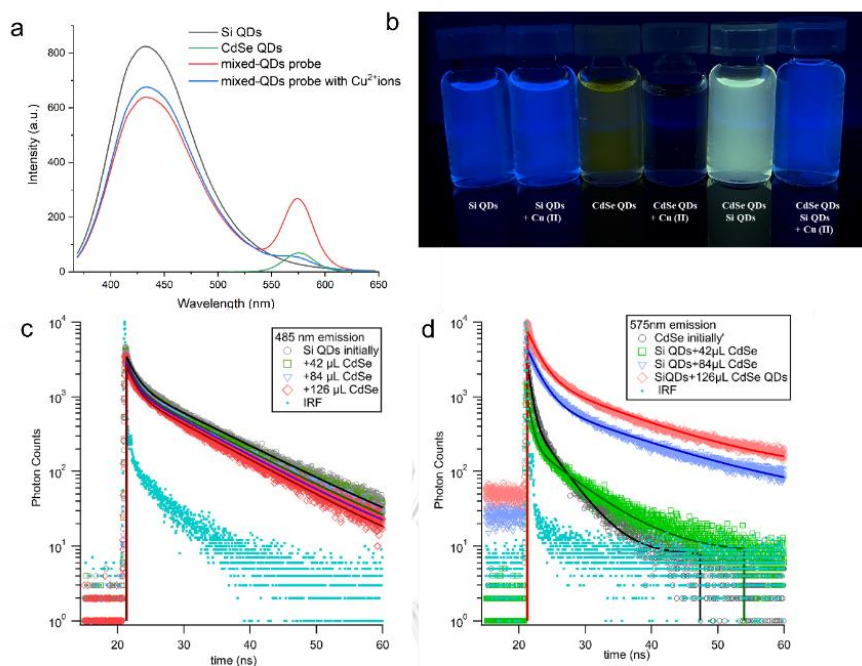
Figure 5.4 The florescence spectra of mixed QDs probe titrate with Cu^{2+} (a), and Si QDs, CdSe QDs, mixed QDs probe in presence and absence of Cu^{2+} under UV lamp (b). Lifetime of Si QDs initially and after addition of CdSe QDs (probe at 485nm) (c), and lifetime of CdSe QDs initially and after addition of CdSe QDs to Si QDs (probe at 575nm). Solid lines represent the fit.
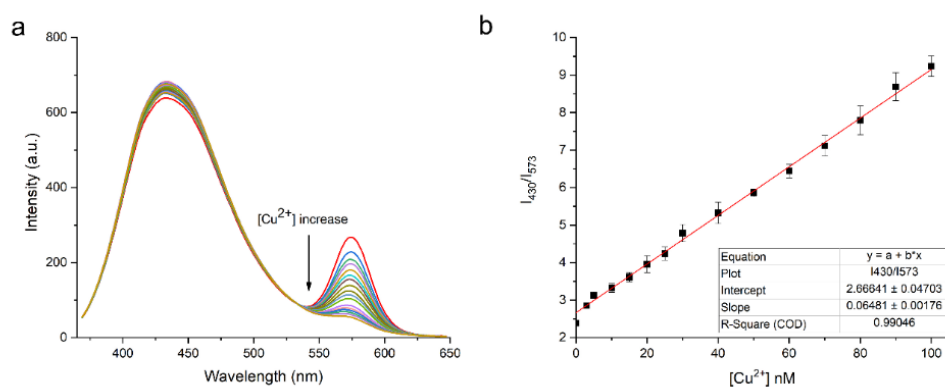
Figure 5.5 The fluorescence titration spectra of the mixed-QDs probe with Cu^{2+} ion (a), and ratio plot of mixed-probe versus $[Cu^{2+}]$ (b).

Since CdSe QDs were dramatically quenched and Si QDs were rarely affected by Cu^{2+} ions, ratiometric fluorescence sensor combining Si QDs and CdSe were

created. A mixed-QD probe was fabricated in 10 mM HEPES buffer (pH = 7.0) by mixing the two QDs in the buffer. The mixed-QDs probe exhibited compatibility between the two aqueous QDs without the induction of precipitation. An FETEM image of the mixed-QDs probe provided information on the particle size and morphology of the probe as homogeneous mixing of the two dots and without any coating or aggregation of mixed dots observed (Figure S5.6) The EDS analysis indicated that this mixed probe contains Cd, Se, Si, S, C, N, and O as shown in Table S5. The emission color of the mixed-QDs probe was yellow-green and was significantly brighter than CdSe QDs, Figure 5.4b.

The mixed-QDs probe showed 2 emission spectra at 430 and 573 nm belonging to Si QDs and CdSe QDs, respectively. However, we observed an enhancement of fluorescence spectra of CdSe QDs at 573 nm when Si QDs are added as shown in Figure 5.4.

Fluorescence resonance energy transfer, FRET, a non-radiative process between two fluorescence molecules was expected to be the reason for enhancement in CdSe fluorescence. FRET relies that the distance between the donor molecule (D) and the acceptor molecule (A) is typically of the order 1-10 nm [65, 86]. For FRET to occur, there are few criteria needed. First, the spectra emission of a donor molecule must overlap with the absorption of an acceptor molecule. Also, the proximity between D and A should be about 10 Å to 100 Å [21-22]. The size of our QDs and the overlap between the emission spectra of Si QDs and absorption spectra of CdSe QDs clearly satisfied the FRET criteria. To confirm the energy transfer between Si QDs and CdSe QDs, fluorescence titration between Si QDs and CdSe QDs was studied in detail as shown in Figure S5.4. We carried out two titration experiments to confirm the energy transfer between Si QDs and CdSe QDs, 1) CdSe QDs were titrated with Si QDs and 2) Si QDs were titrated with CdSe QDs. The results showed that PL intensity of CdSe QDs were enhanced with the increasing amount of Si QDs, and the PL intensity of Si QDs were diminished with the increasing amount of

CdSe QDs, confirming the energy transfer from Si QDs (donor) to CdSe QDs (acceptor) at the excitation of Si QDs (350 nm).

To further confirm the presence of energy transfer, time-resolved (TR) PL measurements were done using 375 nm pulsed laser diode excitation. To separately resolve emission from the Si QDs and CdSe QDs, we probed two different emission channels selected by a monochromator. Figure 5.4c shows the TR-PL signal at 485nm where the emission is dominated by Si QDs, while Figure 5.4d shows the signal at 575nm where the emission is dominated by the CdSe QDs once they are introduced. Both sets of decays were fit with biexponential functions, from which the decay lifetime τ_D is expressed as the amplitude average lifetime. The initial samples of Si QDs (donor) have an amplitude average lifetime of 4.8±0.11 ns, while that of the CdSe (acceptor) was determined to be 1.0±0.12 ns. In the presence of energy transfer from the Si QDs (donor) to the CdSe QDs (acceptor), we will expect the average lifetime of the donor to decrease [87]. Specifically, because the Si QD lifetime is significantly longer than the CdSe QDs lifetime, we expect the lifetime measured at the CdSe QD emission channel to increase when the QDs are additionally excited via energy transfer from the Si QDs, approaching the lifetime recorded at the Si emission channel. Upon addition of CdSe QDs to the Si QDs, the amplitude average lifetime of the Si QDs (donor) continues to decrease with each aliquots addition of CdSe with a corresponding increase in the average lifetime of that of the CdSe QDs (acceptor) as shown in Table S5.1. After the final addition of the CdSe QDs (reaching 0.25 μM CdSe QDs), the amplitude average lifetime of the donor (Si QDs) has decreased to 4.3±0.17 ns while that of the acceptor (CdSe QDs) has increased to 4.1±0.32ns as shown in the Figure 5.4c and Table S5.2. Given the low optical density of the sample, this is clear evidence of non-radiative energy transfer from the Si QDs to the CdSe QDs [88-89]. In addition to this and to corroborate the quenching of the CdSe in the presence of Cu^2 we added successive aliquots of Cu^{2+} to the mixed QD sensor solution. As shown in Figure S5.5, the lifetime of the CdSe QDs continued to diminish with each addition of

Cu^{2+} ions to the mixture. This further confirms that the CdSe QDs is strongly quenched in the presence of Cu^{2+} ions.

Fluorescence technique was used to indicate the detection of Cu^{2+} ions by the mixed QDs probe. The diminish of fluorescence intensity at 573 nm was observed upon the addition of Cu^{2+} ions. This can be attributed to the effect of Cu^{2+} ions on the CdSe QDs surface (Figure 5.5a) The ratiometric plot: I_{430}/I_{573} versus concentration of quencher, Cu^{2+} (Figure 5.5b) showed that there was a linear relationship between the concentration of Cu^{2+} ion and: I_{430}/I_{573} value in the range of 0-100 nM (R^2 = 0.99046). The mixed-QDs probe has a detection limit of 3.89 nM, which was almost 10 times lower than the CdSe (MPA) QDs based sensor published previuosly [73]. The reasons for the high sensitivity of this probe were likely the combination from the sensitivity from using intensity ratio and the increase of CdSe QDs fluorescent signals due to FRET.

Another purpose of implementation of the mixed-QDs probe for sensing Cu^{2+} is the ability for naked eye detection. In the presence of 10 µM of Cu^{2+}, under a UV lamp, the mixed-QDs sensor changes the emission color from yellow-green to blue as shown Figure 5.4b.

4.4 Selectivity study: interference test

In addition to Cu^{2+} ions, the fluorescence quenching of mixed QDs-probe was also evaluated in the presence of some relevant biological cations and cations of environmental problem concerns: $Ag^+, Fe^{3+}, Ni^{2+}, Cr^{3+}, Co^{2+}, Ca^{2+}, Li^+, Mg^{2+}, Sr^{2+}, Al^{3+}, Ba^{2+}, Zn^{2+}, Na^+, K^+, Pb^{2+}, Mn^{2+}, Cd^{2+}$, and Hg^{2+}, as shown in Figure 5.6 The fluorescent ratio (I_{430}/I_{573}) of the mixed-QDs probe increased significantly when exposed to 1 µM Cu^{2+} ions, whereas the exposure to the same concentration of other cations caused slightly changes (~20 times lower), shown in Figure 5.6a. In the presence of 1 µM Cu^{2+} ions, other cations did not change the intensity ratio as well. These observations

indicated the good selectivity of Cu^{2+} ions compared with the other competitive cations.

The selectivity of the mixed-QDs probe to Cu^{2+} ions is due to the reasons mentioned earlier including the deposition of CuS and/or substitution of Cd^{2+} ion by Cu^{2+} ion leading to the non-radiative recombination of exciton. From the hard-soft acid-base theory, Cu^{2+} ion has Pearson border acid character which has a strong interaction with thiol groups [23]. Other metals with hard and borderline acid characters could bind to both carboxylate group of MPA on CdSe QDs and citrate group on Si QDs, and did not lead to the deposition of metal salts on QDs surface. Only in the presence of Cu^{2+} ions, the thiol group of MPA will react with Cu^{2+} ions to form CuS [70] leading to the quenching of luminescence [76].

To demonstrate that the mixed-QDs probe can be used as the naked eye detection with selectivity to Cu^{2+}, Figure 5.6b illustrates the changes in emission color comparing of Si QDs, CdSe, QDs, mixed-QDs probe (with and without Cu). The yellow-green emission of probe completely turn to blue emission upon the addition of Cu^{2+} while it is remaining yellow-green by the addition of the other cations.
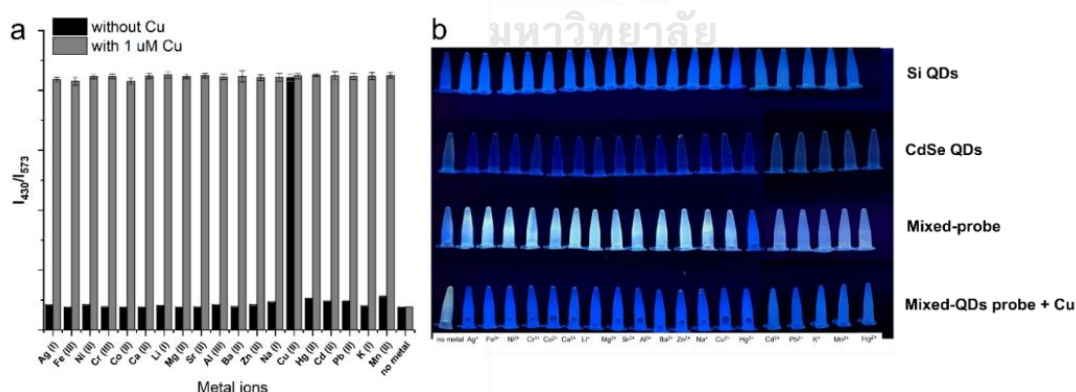
Figure 5.6 The selectivity study of mixed-QDs probe comparing the absence and internal Cu^{2+} adding (a), and interferences study under UV-lamp (ex 365 nm) (b).

5. Conclusion

This work has demonstrated the ratiometric fluorescence sensor for rapid, sensitive, and selective to Cu^{2+} ions using the mixed-QDs probe in an aqueous solution. The mixed-QDs probe consists of two types of QDs are CdSe QDs and Si QDs without any modification on the surface. Mixed QDs probe has good solubility in aqueous without any accumulation. The yellow-green emission of mixed-QDs probe originated from the yellow-emitting CdSe QDs and blue emitting Si QDs. In the presence of Cu^{2+} ions, the emission color would turn to blue. The detection limit was 3.89 nmol L^{-1} for Cu^{2+} ions with the linear range from 0-100 nmol L^{-1} (R^2 = 0.99046). The mixed-QDs probe has a good sensitivity and selectivity toward to the biological relevant cations and cations of environmental concern: Ag^+, Fe^{3+}, Ni^{2+}, Cr^{3+}, Co^{2+}, Ca^{2+}, Li^+, Mg^{2+}, Sr^{2+}, Al^{3+}, Ba^{2+}, Zn^{2+}, Na^+, K^+, Pb^{2+}, Mn^{2+}, Cd^{2+}, and Hg^{2+}. The detection limit and linear range of this mixed-QDs probe are comparable with other QDs probes reported previously, with the advantage of the large range of other metal cations that this probe can tolerate as shown in Table S6.

The mixed-QDs probe demonstrates the ratiometric fluorescent probe with only QDs-based fluorophores. Photostability, sensitivity, selectivity and ability for naked eye detection of Cu^{2+} could allow this probe system to be further developed for use in analysis of water samples and biological specimens.

6. Acknowledgements

Supplementary information II

Experimental

Chemicals

All chemicals were used without any furthur purification. Trisodium citrate dehydrate 99%, 3-(aminopropyl)trimethoxylsilane 97% (APTES) 3-mercatopropionic acid 98% (MPA), Hydrazine hydrate 99% ($N_2H_4 \cdot H_2O$), sodium hydroxide, (NaOH), N-[2-hydroxylethyl] piperazine-N'- [2-ethane-sulfonic acid] 99+ % (HEPES) were purchased from Sigma Aldrich. Cadmium chloride anhydrous, $CdCl_2$ > 99%, was from Fluka. Sodium selenite anhydrous 99% (Na_2SeO_3) was from Alfa Aesar. All the metal salts were analytical grade and purchased from Ajax Finechem, Thermo Fisher Scientific. Ultrapure water is used throughout (Milli-Q pure system, Millipore).

Instrumentation

Absorption spectra were recorded using a HP 8453 UV-VIS spectrophotometer. Fluorescence spectra measurements were done with a Cary Eclipse Fluorescence spectrophotometer at excitation = 350 nm. PerkinElmer, EnSight multimode microplate reader was used to analyze fluorescence intensity in selectivity study. Fluorescence lifetime of QDs were measured using Horiba DeltaFlex spectrophotometer Field emission transmission electron microscopic (FETEM) images of the quantum dots were captured using field emission transmission electron microscope: JEOL, JEM-3100F after depositing them on carbon-coated Cu grids. The elemental composition analysis was carried out by X-ray photoelectron spectrometer, XPS; AXIS ULTRADLD, Kratos analytical, Manchester UK. Fourier Transform Infrared, FTIR spectra were recorded by Thermo Scientific, Nicolet iS50 FTIR.
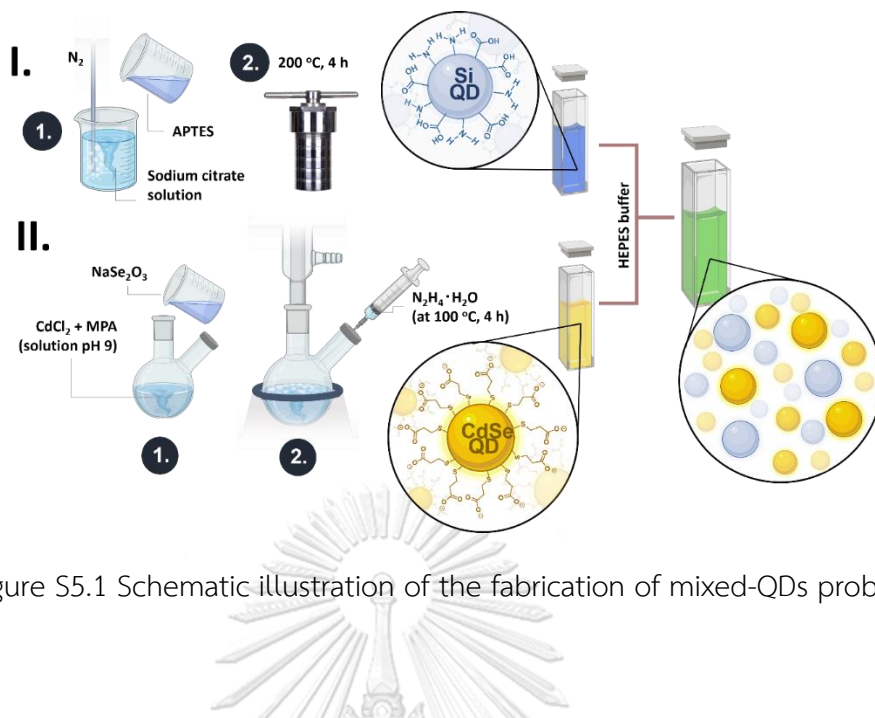
Figure S5.1 Schematic illustration of the fabrication of mixed-QDs probe
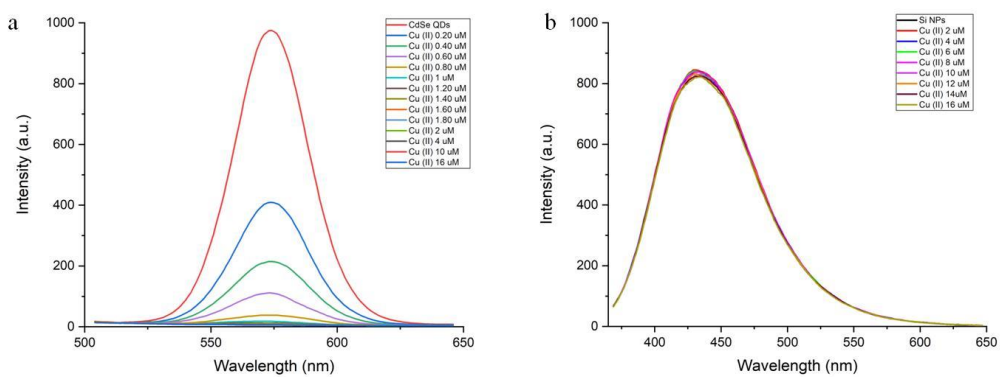
Figure S5.2 The fluorescence spectra of CdSe QDs (a) and Si QDs (b) while adding Cu^{2+} ions.
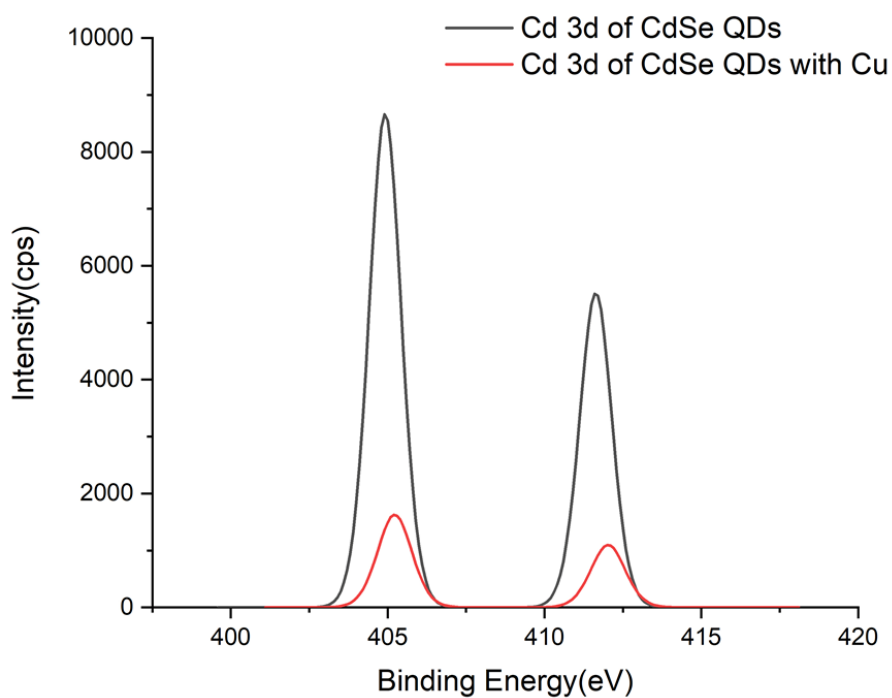
Figure S5.3 High-resolution XPS spectra of CdSe QDs at Cd 3d.
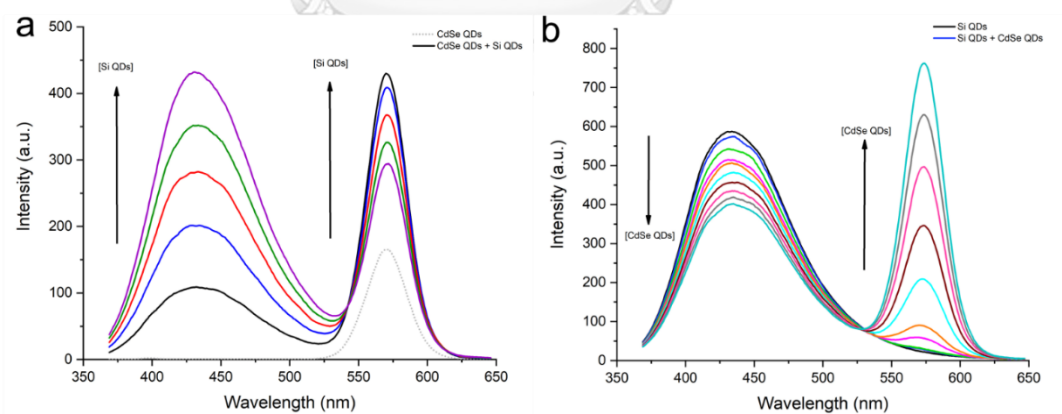
Figure S5.4 The fluorescence titration spectra of mixed QDs probe compared to those origin spectra.
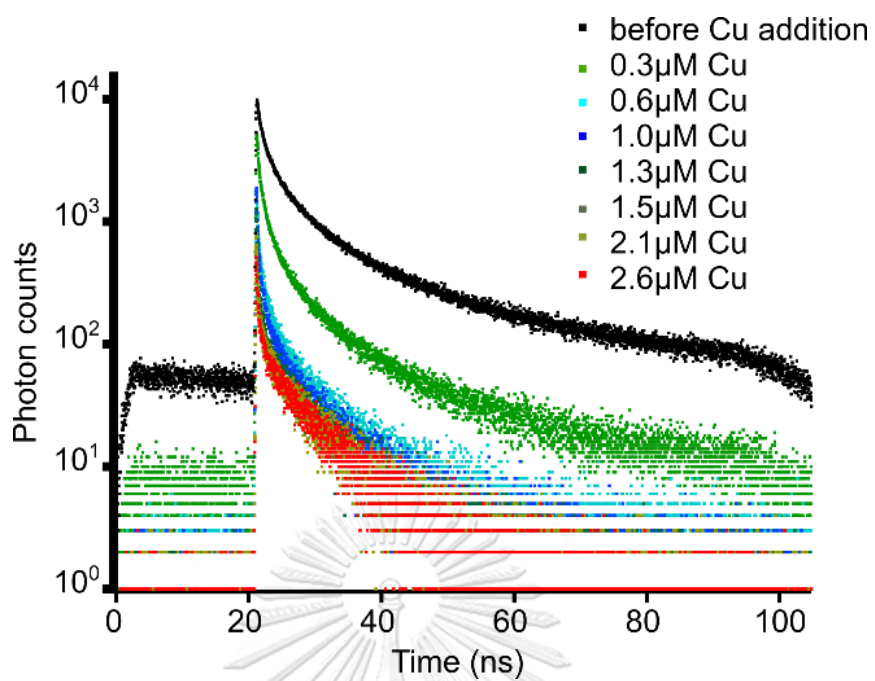
Figure S5.5 The fluorescence lifetime of CdSe QDs and Si QDs mixture before and after addition of Cu^{2+} (probe at 575nm).
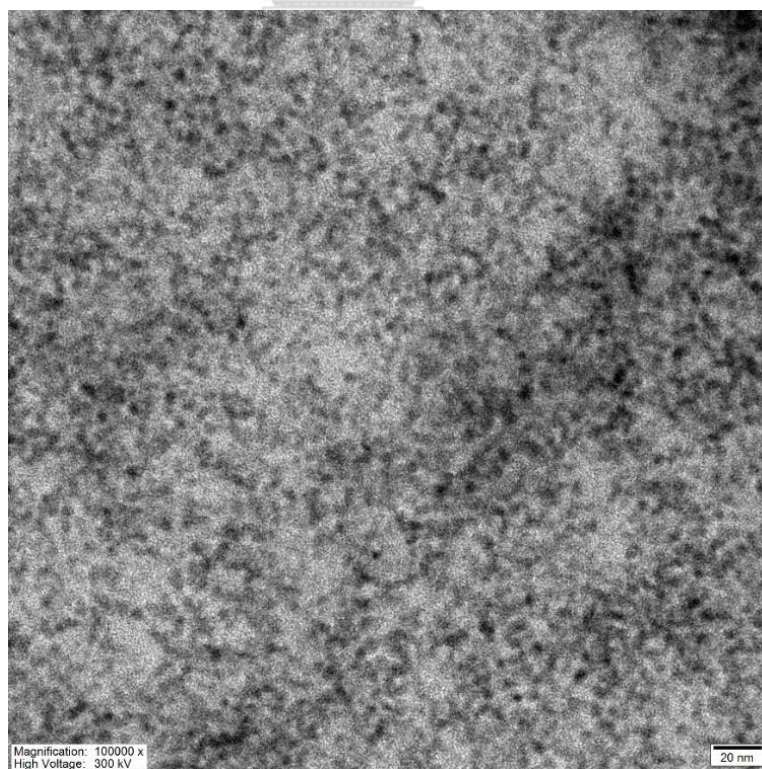
Figure S5.6 The FETEM image of the mixed-QDs probe.
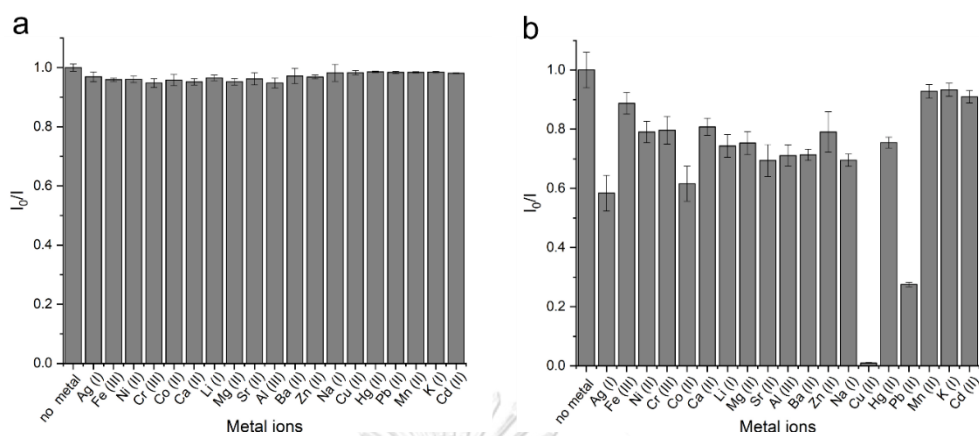
Figure S5.7 Effect of other cations on CdSe QD (a) and Si QDs (b).
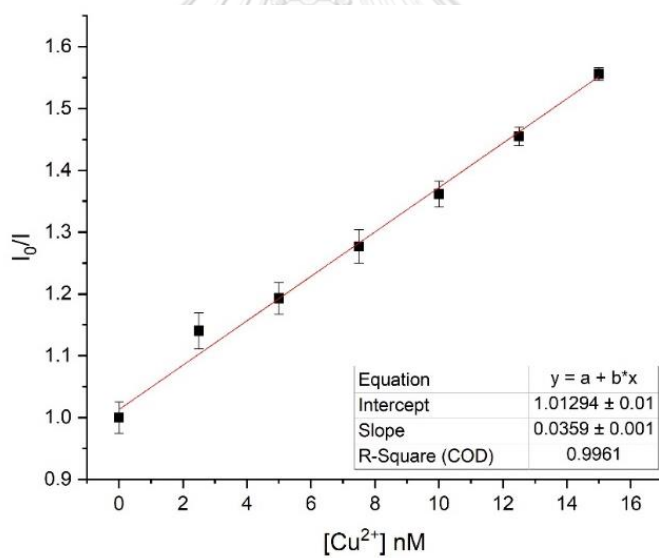
Figure S5.8 Stern-Volmer's plot of CdSe QDs with Cu^{2+}

Table S5.1 Amplitude average lifetime of Si QDs initially and after addition of CdSe QDs (probe at 485nm). Uncertainties in TR-PL parameters are 95% confidence intervals as reported by Horiba DeltaFlex software

	Si QDs initially	Si QDs+ 42uL CdSe QDs	Si QDs+ 84uL CdSe QDs	Si QDs+ 126uL CdSe QDs
τ avg (ns)	4.8±0.11	4.7±0.12	4.5±0.12	4.3±0.17
Chi Sq. (χ^2)	1.5	1.6	1.5	1.5

Table S5.2 Amplitude average lifetime of CdSe QDs initially and after addition of CdSe QDs to Si QDs (probe at 575nm). Uncertainties in TR-PL parameters are 95% confidence intervals as reported by Horiba DeltaFlex software

	CdSe QDs	Si QDs + 42uL CdSe QDs	Si QDs + 84uL CdSe QDs	Si QDs + 126uL CdSe QDs
τ avg (ns)	1.0±0.12	1.8±0.24	4.1±0.29	4.1±0.32
Chi Sq. (χ^2)	1.9	1.3	2.8	2.3

Table S5.3 Elemental analysis of Si QDs by FETEM

Element	Weight %	Atomic %
C	49.51	60.82
N	2.67	2.81
O	28.37	26.16
Si	19.45	10.21

Table S5.4 Elemental analysis of CdSe QDs by FETEM

Element	Weight %	Atomic %
C	55.62	75.30
O	11.82	12.02
S	21.53	10.92
Cd	8.18	1.18
Se	2.84	0.59

Table S5.5 Elemental analysis of mixed -QDs probe by FETEM

Element	Weight %	Atomic %
C	21.65	38.10
N	4.20	6.35
O	22.49	29.72
Si	23.81	17.93

S	5.46	3.60
Se	1.22	0.33
Cd	21.17	3.98

Table S5.6 shows the comparison of Cu sensing based on quantum dots

Entry	Sensor	Analyze	LOD (nM)	Reported tolerated metal ions	Linear range	REF
1	CdSe/ZnS (BSA)	Cu^{2+} Fe^{3+}	10	Ca^{2+}, K^+, Na^+, Mg^{2+}, Mn^{2+}, Zn^{2+}, Fe^{3+}	0.01-2µM	[74]
2	CdSe/ZnS (CTAB)	Cu^{2+}	0.15	Zn^{2+}, Pb^{2+}, In^{3+}, Fe^{3+}, Co^{2+}, Cd^{2+}, Ca^{2+}; Hg^{2+}, Ag^+	N/A	[78]
3	CdTe(TGA)	Cu^{2+}	0.04	Pb^{2+}, Hg^{2+}, Ca^{2+}, Zn^{2+}, Cd^{2+}, Mg^{2+}, K^+, Na^+, Ag^+, Fe^{3+}	0.25-617.53 nM	[75]
4	CdTe(TGA) + MOF	Cu^{2+}	4.09	Mg^{2+}, Pb^{2+}, Co^{2+}, Ba^{2+}, $Mn^{2=}$, Fe^{3+}, Cr^{6+}, Zr^{4+}, Ca^{2+}, Ag^+, Hg^{2+}	4.0-40.0 ng/ml	[70]

5	CdSeTe QD (cys)	Cu^{2+}	7.1	$Pb^{2+},Fe2+ K^+$, Na^+, Mg^{2+}, Al^{3+}, Ca^{2+}, Zn^{2+}.	20nM-2uM	[20]
6	CdTe/ZnS	Cu^{2+}	1.50	Ag^+, Hg^{2+}, Co^{2+}, Ba^{2+}, Zn^{2+}, Al^{3+}, Cd^{2+}, Ni^{2+}, Ca^{2+}, Mg^{2+}, Mn^{2+}, Pb^{2+}, Na^+, K^+, Cr^{3+}, Fe^{2+}, Fe^{3+}	2.5 nM-1.75 µM	[33]
7	CdSe (MPA)	Cu^{2+}	30	Fe^{3+}, Zn^{2+}, Ag^+, Mn^{2+}, Co^{2+}, Hg^{2+}, Pb^{2+}	30 nM-3 µM	[73]
8	ZnSe (MPA)	Cu^{2+}	170	Al^{3+}, Ba^{2+}, Ca^{2+}, Fe^{3+}, K^+, Mg^{2+}, Mn^{2+}, Na^+, NH_4^+, Zn^{2+}	0.059 – 9.84 µM	[76]
9	CdS QDs	Cu^{2+}	10	K^+, Na^+, Ca^{2+}, Mg^{2+}, Zn^{2+}, Mn^{2+}, Fe^{3+}, Co^{2+}	0.02 – 2.0 µM	[45]
10	Mixed-QDs probe (CdSe-Si QDs)	Cu^{2+}	3.89	Ag^+, Fe^{3+}, Ni^{2+}, Cr^{3+}, Co^{2+}, Ca^{2+}, Li^+, Mg^{2+}, Sr^{2+}, Al^{3+}, Ba^{2+}, Zn^{2+}, Na^+, K^+, Pb^{2+}, Mn^{2+}, Cd^{2+}, Hg^{2+}	0-100 nM	**This work**

CHAPTER VI

CONCLUSION

This thesis contains two main projects, which are i) the detection of urate in an aqueous solution called "dual-dyes probe" and ii) the detection of Cu^{2+} in an aqueous solution called "mixed-QDs probe" and. Both sensing probe are ratiometric fluorescence probe with the fluorescence resonance energy transfer with facile, sensitive, selective, fast, simple, naked-eyes tool for analyze.

The aqueous-based detection probe of Cu^{2+} called 'mixed-QDs probe' was successfully fabricated. This probe consists of 2 main QDs are Si QDs and CdSe QDs. There are the resonance energy transfer between these 2 QDs and a ratiometric fluorescence sensing system. The time-resolved fluorescence confirmed the energy transfer between Si QDs and CdSe QDs. X-ray photoelectron spectrometer (XPS) indicated the quenching mechanism of Cu^{2+} to the mixed-QDs probe. This probe has a high selectivity toward Cu^{2+} in the presence of the other biological relevant metals; Ag^+, Fe^{3+}, Ni^{2+}, Cr^{3+}, Co^{2+}, Ca^{2+}, Li^+, Mg^{2+}, Sr^{2+}, Al^{3+}, Ba^{2+}, Zn^{2+}, Na^+, K^+, Pb^{2+}, Mn^{2+}, Cd^{2+}, and Hg^{2+}. It is also sensitive to Cu^{2+}, provides the low detection limit as 3.89 nmol L^{-1} with linear range from 0-100 nmol L^{-1} and R^2 = 0.99046. Moreover, this probe showed the fluorescence color changing from blue to yelow-green upon the addition of Cu^{2+} which can be the naked-eyes detection tool.

Urate sensing probe in an aqueous solution has been developed with the advantages of ratiometric system, FRET, and IDA. This ratiometric fluorescence sensing probe called 'dual-dyes probe', consisting of 3 main components are quinine sulfate dyes, eosin Y dyes, and dinuclear copper (II) complex, Cu_2L. The dual-dyes probe is sensitive to 3 main anions are urate, oxalate, and citrate over the other anion that can be found in urine and other biological samples including potassium sulfate, sodium chloride, magnesium sulfate, urea, ammonium chloride, sodium

dihydrogen orthophosphate, calcium chloride, sodium sulfate, creatinine, di-potassium hydrogen phosphate, terephthalate, malonate, fumarate, succinate, carbonate, ascorbate, phosphate, and maleate. The detection limit equal to 0.0699, 0.3790, and 1.0472 µmol L^{-1} for urate, oxalate, and citrate, respectively. The ratiometric fluorescence study on the synthetic urine and patient mimics synthetic urine claimed the distinguish of urate from oxalate and citrate ions by the optimize dilution factor according to the amount of each anion in normal urine found. Beside the presence of urate, the emission color of dual dyes probe was obviously changed from blue to green which is very compactable for the onsite purpose in the future.

จุฬาลงกรณ์มหาวิทยาลัย
CHULALONGKORN UNIVERSITY

REFERENCES

1.   Hontz, D.; Hensley, J.; Hiryak, K.; Lee, J.; Luchetta, J.; Torsiello, M.; Venditto, M.; Lucent, D.; Terzaghi, W.; Mencer, D.; Bommareddy, A.; VanWert, A. L., A Copper(II) Macrocycle Complex for Sensing Biologically Relevant Organic Anions in a Competitive Fluorescence Assay: Oxalate Sensor or Urate Sensor? *ACS Omega* **2020,** *5* (31), 19469-19477.

2.   Mansur, H. S., Quantum dots and nanocomposites. *Wiley Interdiscip Rev Nanomed Nanobiotechnol* **2010,** *2* (2), 113-29.

3.   Frasco, M. F.; Chaniotakis, N., Semiconductor quantum dots in chemical sensors and biosensors. *Sensors (Basel)* **2009,** *9* (9), 7266-86.

4.   Xing, B.; Li, W.; Dou, H.; Zhang, P.; Sun, K., Systematic Study of the Properties of CdSe Quantum Dots Synthesized in Paraffin Liquid with Potential Application in Multiplexed Bioassays. *The Journal of Physical Chemistry C* **2008,** *112* (37), 14318-14323.

5.   Chu, M.; Wu, F.; Zhang, Q.; Liu, T.; Yu, Y.; Ji, A.; Xu, K.; Feng, Z.; Zhu, J., A novel method for preparing quantum dot nanospheres with narrow size distribution. *Nanoscale* **2010,** *2* (4), 542-7.

6.   Callen, J. F.; Raymo, F. M., *Technology and commercial apllications quantum dot sensors*. Pan Stanford: Pan Stanford publishing Pte. Ltd.

7.   Chen, X.; Tang, Y.; Cai, B.; Fan, H., 'One-pot' synthesis of multifunctional GSH–CdTe quantum dots for targeted drug delivery. *Nanotechnology* **2014,** *25* (23), 235101.

8.   Chen, A.; Peng, X.; Pan, Z.; Shao, K.; Wang, J.; Fan, M., Visual Assay of Glutathione in Vegetables and Fruits Using Quantum Dot Ratiometric Hybrid Probes. *J Agric Food Chem* **2018,** *66* (25), 6431-6438.

9.   Zhang, X.; Chen, X.; Kai, S.; Wang, H. Y.; Yang, J.; Wu, F. G.; Chen, Z., Highly sensitive and selective detection of dopamine using one-pot synthesized highly photoluminescent silicon nanoparticles. *Anal Chem* **2015,** *87* (6), 3360-5.

10.   Zhong, Y.; Peng, F.; Bao, F.; Wang, S.; Ji, X.; Yang, L.; Su, Y.; Lee, S. T.; He, Y., Large-scale aqueous synthesis of fluorescent and biocompatible silicon nanoparticles and their use as highly photostable biological probes. *J Am Chem Soc* **2013,** *135* (22), 8350-6.

11.   Li, Z.; Ren, X.; Hao, C.; Meng, X.; Li, Z., Silicon quantum dots with tunable emission synthesized via one-step hydrothermal method and their application in alkaline phosphatase detection. *Sensors and Actuators B: Chemical* **2018,** *260*, 426-431.

12.   Alivisatos, P.; Gu, W.; Larabell, C., Quantum dots as cellular probes. *Annu. Rev. Biomed. Eng.* **2005,** *7*, 55-76.

13.   Fu, A.; Gu, W.; Larabell, C.; Alivisatos, P., Semiconductor nanocrystals for biological imaging. *Curr. Opin. Neurobiol.* **2005,** *15*, 568-575.

14.   Zrazhevskiy, P.; Senawb, M.; Gao, X., Designing multifunctional quantum dots for bioimaging, detection, and drug delivery. *Chem. Soc. Rev.* **2010,** *39*, 4326-4354.

15.   Walling, A. M.; Novak, A. J.; Shepard, J. R. E., Quantum dots for live cell and in vivo iImaging. *Int. J. Mol. Sci.* **2009,** *10*, 441-491.

16.   Zhu, H.; Hu, M. Z.; Shao, L.; Yu, K.; Dabestani, R.; Zaman, M. B.; Liao, S., Synthesis and Optical Properties of Thiol Functionalized CdSe/ZnS (Core/Shell) Quantum Dots by Ligand Exchange. *Journal of Nanomaterials* **2014,** *2014*, 1-14.

17.   Zhou, Q.; Li, Z.; Wang, Q.; Peng, L.; Luo, S.; Gu, F. L., Polymer-capped CdSe/ZnS quantum dots for the sensitive detection of Cu(2+) and Hg(2+) and the quenching mechanism. *Anal Methods* **2021,** *13* (20), 2305-2312.

18. Sun, Q.; Fu, S.; Dong, T.; Liu, S.; Huang, C., Aqueous synthesis and characterization of TGA-capped CdSe quantum dots at freezing temperature. *Molecules* **2012**, *17* (7), 8430-8.

19. Granados-Oliveros, G.; Pineros, B. S. G.; Calderon, F. G. O., CdSe/ZnS quantum dots capped with oleic acid and L-glutathione: Structural properties and application in detection of Hg^{2+}. *Journal of Molecular Structure* **2022**, *1254*, 132293.

20. Liang, G. X.; Liu, H. Y.; Zhang, J. R.; Zhu, J. J., Ultrasensitive Cu^{2+} sensing by near-infrared-emitting CdSeTe alloyed quantum dots. *Talanta* **2010**, *80* (5), 2172-6.

21. Duong, H. D.; Rhee, J. I., Development of Ratiometric Fluorescence Sensors Based on CdSe/ZnS Quantum Dots for the Detection of Hydrogen Peroxide. *Sensors (Basel)* **2019**, *19* (22).

22. Marandi, M.; Nazari, M., Application of TiO2 hollow spheres and ZnS/SiO2 double-passivaiting layers in the photoanode of the CdS/CdSe QDs sensitized solar cells for the efficiency enhancement. *Solar Energy* **2021**, *216*, 48-60.

23. He, Y. F.; Chen, J. W.; An, C. Z.; Hou, X. L.; Zhong, Z. T.; Li, C. Q.; Chen, W.; Liu, B.; Zhao, Y. D., Labeling of liver cells with CdSe/ZnS quantum dot-based fluorescence probe below freezing point. *Spectrochim Acta A Mol Biomol Spectrosc* **2021**, *263*, 120203.

24. Deng, B.-Y.; Wu, J.; Liu, J.; Ren, Y.-Y.; Wang, F., Facile passivation of yellow light-emitting CdSe QDs by polyethyleneimine in water to achieve bright white light emission. *Materials Advances* **2021**, *2* (22), 7384-7388.

25. Luo, L.; Song, Y.; Zhu, C.; Fu, S.; Shi, Q.; Sun, Y.-M.; Jia, B.; Du, D.; Xu, Z.-L.; Lin, Y., Fluorescent silicon nanoparticles-based ratiometric fluorescence immunoassay for sensitive detection of ethyl carbamate in red wine. *Sensors and Actuators B: Chemical* **2018**, *255*, 2742-2749.

26. Sharma, B.; Tanwar, S.; Sen, T., One Pot Green Synthesis of Si Quantum Dots and Catalytic Au Nanoparticle–Si Quantum Dot Nanocomposite. *ACS Sustainable Chemistry & Engineering* **2019**, *7* (3), 3309-3318.

27. Azmi, N. E.; Ramli, N. I.; Abdullah, J.; Abdul Hamid, M. A.; Sidek, H.; Abd Rahman, S.; Ariffin, N.; Yusof, N. A., A simple and sensitive fluorescence based biosensor for the determination of uric acid using H2O2-sensitive quantum dots/dual enzymes. *Biosens Bioelectron* **2015**, *67*, 129-33.

28. Hussain, S. A., *An introduction to fluorescence resonance energy transfer (FRET)*. 2009; Vol. 132.

29. A. Kratz; M. Ferraro; P. M. Sluss; Lewandrowski, K. B., Laboratory Reference Values. *N. Engl. J Med.* **2004**, *351*, 1548-1563.

30. Shamirian, A.; Ghai, A.; Snee, P. T., QD-Based FRET Probes at a Glance. *Sensors (Basel)* **2015**, *15* (6), 13028-51.

31. Nguyen, B. T.; L, S.; Wiskur; Anslyn, E. V., Using indicator-displacement assays in test strips and to follow reaction kinetics. *Org. Lett.* **2004**, *6*, 2499-2501.

32. Nguyen, B. T.; Anslyn, E. V., Indicator–displacement assays. *Coord. Chem. Rev.* **2006**, *250*, 3118-3127.

33. Bian, W.; Wang, F.; Zhang, H.; Zhang, L.; Wang, L.; Shuang, S., Fluorescent probe for detection of Cu^{2+} using core-shell CdTe/ZnS quantum dots. *Luminescence* **2015**, *30* (7), 1064-70.

34. Rhaman, M. M.; Fronczek, F. R.; Powell, D. R.; Hossain, M. A., Colourimetric and fluorescent detection of oxalate in water by a new macrocycle-based dinuclear nickel complex: a remarkable red shift of the fluorescence band. *Dalton Trans* **2014**, *43* (12), 4618-21.

35. Jaeger, P.; Robertson, W. G., Role of dietary intake and intestinal absorption of oxalate in calcium stone formation. *Nephron Physiol* **2004**, *98* (2), p64-71.

36. Hu, M.; Feng, G., Highly selective and sensitive fluorescent sensing of oxalate in water. *Chem Commun (Camb)* **2012**, *48* (55), 6951-3.

37. Tanga, L.; Zhaoa, G.; Tang, B., Colorimetric recognition of oxalate in water by a new carbazole-Zn(II) based chemosensing ensemble. *J. Chem. Res.* **2013**, 542–545.

38. Worramongkona, P. S., K.; Phansomboon, P.; Ratnarathorn, N.; Chailapakul, O.; Dungchai, W., A Simple paper-based colorimetric device for rapid and sensitive urinary oxalate determinations. *Anal. Sci.* **2018,** *34*, 103-108.

39. Inoue, K.; Aikawa, S.; Fukushima, Y., Colorimetric detection of oxalate in aqueous solution by a pyrogallol red-based Cu^{2+} complex. *J. Lumin.* **2018,** *33*, 277-281.

40. Ding, Y.; Sun, H.; Liu, D.; Liu, F.; Wang, D.; Jiang, Q., Water-soluble, high-quality ZnSe@ZnS core/shell structure nanocrystals. *J. Chin. Adv. Mat. Soc.* **2013,** *1*, 56-64.

41. Soheyli, E.; Sahraei, R.; Nabiyouni, G.; Nazari, F.; Tabaraki, R.; Ghaemi, B., Luminescent, low-toxic and stable gradient-alloyed Fe:ZnSe(S)@ZnSe(S) core:shell quantum dots as a sensitive fluorescent sensor for lead ions. *Nanotechnology* **2018,** *29*, 1-47.

42. Shu, C.; Huang, B.; Chen, X.; Wang, Y.; Li, X.; Ding, L.; Zhong, W., Facile synthesis and characterization of water soluble ZnSe/ZnS quantum dots for cellar imaging. *Spectrochim Acta A Mol Biomol Spectrosc* **2013,** *104*, 143-9.

43. Curcio, R.; Stettler, H.; Suter, P. M.; Aksozen, J. B.; Saleh, L.; Spanaus, K.; Bochud, M.; Minder, E.; von Eckardstein, A., Reference intervals for 24 laboratory parameters determined in 24-hour urine collections. *Clin Chem Lab Med* **2016,** *54* (1), 105-16.

44. Epuran, C.; Fratilescu, I.; Anghel, D.; Birdeanu, M.; Orha, C.; Fagadar-Cosma, E., A Comparison of Uric Acid Optical Detection Using as Sensitive Materials an Amino-Substituted Porphyrin and Its Nanomaterials with CuNPs, PtNPs and Pt@CuNPs. *Processes* **2021,** *9* (11), 2072.

45. Wang, G. L.; Dong, Y. M.; Li, Z. J., Metal ion (silver, cadmium and zinc ions) modified CdS quantum dots for ultrasensitive copper ion sensing. *Nanotechnology* **2011,** *22* (8), 085503.

46. Income, K.; Ratnarathorn, N.; Khamchaiyo, N.; Srisuvo, C.; Ruckthong, L.; Dungchai, W., Disposable Nonenzymatic Uric Acid and Creatinine Sensors Using muPAD Coupled with Screen-Printed Reduced Graphene Oxide-Gold Nanocomposites. *Int J Anal Chem* **2019,** *2019*, 3457247.

47. Rezaei, H.; Jouyban, A.; Rahimpour, E., Development of a new method based on gold nanoparticles for determination of uric acid in urine samples. *Spectrochim Acta A Mol Biomol Spectrosc* **2022,** *272*, 120995.

48. Zhang, T.; Sun, X.; Liu, B., Synthesis of positively charged CdTe quantum dots and detection for uric acid. *Spectrochim Acta A Mol Biomol Spectrosc* **2011,** *79* (5), 1566-72.

49. Li, F.; He, T.; Wu, S.; Peng, Z.; Qiu, P.; Tang, X., Visual and colorimetric detection of uric acid in human serum and urine using chitosan stabilized gold nanoparticles. *Microchemical Journal* **2021,** *164*, 105987.

50. Islam, M. N.; Ahmed, I.; Anik, M. I.; Ferdous, M. S.; Khan, M. S., Developing Paper Based Diagnostic Technique to Detect Uric Acid in Urine. *Front Chem* **2018,** *6*, 496.

51. He, Y.; Qi, F.; Niu, X.; Zhang, W.; Zhang, X.; Pan, J., Uricase-free on-demand colorimetric biosensing of uric acid enabled by integrated CoP nanosheet arrays as a monolithic peroxidase mimic. *Anal Chim Acta* **2018,** *1021*, 113-120.

52. Lin, Z.; Ma, Q.; Fei, X.; Zhang, H.; Su, X., A novel aptamer functionalized CuInS2 quantum dots probe for daunorubicin sensing and near infrared imaging of prostate cancer cells. *Anal Chim Acta* **2014,** *818*, 54-60.

53. Zhu, H.; Hu, M. Z.; Shao, L.; Yu, K.; Dabestani, R.; Zaman, B.; Liao, S., Synthesis and Optical Properties of Thiol Functionalized CdSe/ZnS (Core/Shell) Quantum Dots by Ligand Exchange. *Journal of Nanomaterials* **2014,** *2014*, 1-14.

54. Kim, J. S.; Cho, B.; Cho, S. G.; Sohn, H., Silicon quantum dot sensors for an explosive taggant, 2,3-dimethyl-2,3-dinitrobutane (DMNB). *Chem Commun (Camb)* **2016,** *52* (53), 8207-10.

55.   Sha, R.; Vishnu, N.; Badhulika, S., MoS2 based ultra-low-cost, flexible, non-enzymatic and non-invasive electrochemical sensor for highly selective detection of Uric acid in human urine samples. *Sensors and Actuators B: Chemical* **2019**, *279*, 53-60.

56.   Luigi Fabbrizzi, N. M., Floriana Stomeo, and Angelo Taglietti, Pyrophosphate Detection in Water by Fluorescence Competition Assays: Inducing Selectivity through the Choice of the Indicato. **2002**.

57.   Matiel, D. C. a. A. E., THE SYNTHESIS OF NEW BINUCLEATING POLYAZA MACROCYCLIC AND MACROBICYCLIC LIGANDS: DIOXYGEN AFFINITIES OF THE COBALT COMPLEXES. **1991**.

58.   Sarigul, N.; Korkmaz, F.; Kurultak, I., A New Artificial Urine Protocol to Better Imitate Human Urine. *Sci Rep* **2019**, *9* (1), 20159.

59.   Chu, B.; Wang, H.; Song, B.; Peng, F.; Su, Y.; He, Y., Fluorescent and Photostable Silicon Nanoparticles Sensors for Real-Time and Long-Term Intracellular pH Measurement in Live Cells. *Anal Chem* **2016**, *88* (18), 9235-42.

60.   Ki, D.; Sohn, H., Water Soluble Silicon Quantum Dots Grafted with Amoxicillin as a Drug Delivery System. *J Nanosci Nanotechnol* **2020**, *20* (8), 4624-4628.

61.   Dhenadhayalan, N.; Lee, H. L.; Yadav, K.; Lin, K. C.; Lin, Y. T.; Chang, A. H., Silicon Quantum Dot-Based Fluorescence Turn-On Metal Ion Sensors in Live Cells. *ACS Appl Mater Interfaces* **2016**, *8* (36), 23953-62.

62.   Zhang, Q.; Zhang, Y.; Huang, S.; Huang, X.; Luo, Y.; Meng, Q.; Li, D., Application of carbon counterelectrode on CdS quantum dot-sensitized solar cells (QDSSCs). *Electrochemistry Communications* **2010**, *12* (2), 327-330.

63.   Poly, L. P.; Mace, B.; Kottokkaran, R.; Bagheri, B.; Noack, M.; Dalal, V. In *Novel CdSe Solar Cell*, 2021 IEEE 48th Photovoltaic Specialists Conference (PVSC), 20-25 June 2021; 2021; pp 0443-0446.

64.   Speranskaya, E. S.; Beloglazova, N. V.; Lenain, P.; De Saeger, S.; Wang, Z.; Zhang, S.; Hens, Z.; Knopp, D.; Niessner, R.; Potapkin, D. V.; Goryacheva, I. Y., Polymer-coated fluorescent CdSe-based quantum dots for application in immunoassay. *Biosens Bioelectron* **2014**, *53*, 225-31.

65.   Medintz, I. L.; Mattoussi, H., Quantum dot-based resonance energy transfer and its growing application in biology. *Phys Chem Chem Phys* **2009**, *11* (1), 17-45.

66.   Tomokazu, K.; Nayuta, F.; Takeshi, F.; Miho, S., CdSe/ZnS Quantum Dots Conjugated with a Fluorescein Derivative: a FRET-based pH Sensor for Physiological Alkaline Conditions. *ANALYTICAL SCIENCES* **2014**, *30*.

67.   Jin, T.; Sasaki, A.; Kinjo, M.; Miyazaki, J., A quantum dot-based ratiometric pH sensor. *Chem Commun (Camb)* **2010**, *46* (14), 2408-10.

68.   Jose, A. R.; Sivasankaran, U.; Menon, S.; Kumar, K. G., A silicon nanoparticle based turn off fluorescent sensor for sudan I. *Analytical Methods* **2016**, *8* (28), 5701-5706.

69.   Soheyli, E.; Sahraei, R.; Nabiyouni, G.; Nazari, F.; Tabaraki, R.; Ghaemi, B., Luminescent, low-toxic and stable gradient-alloyed Fe:ZnSe(S)@ZnSe(S) core:shell quantum dots as a sensitive fluorescent sensor for lead ions. *Nanotechnology* **2018**, *29* (44), 445602.

70.   Yang, Y.; Liu, W.; Cao, J.; Wu, Y., On-site, rapid and visual determination of Hg(2+) and Cu(2+) in red wine by ratiometric fluorescence sensor of metal-organic frameworks and CdTe QDs. *Food Chem* **2020**, *328*, 127119.

71.   Zhang, J.; Yu, S. H., Highly photoluminescent silicon nanocrystals for rapid, label-free and recyclable detection of mercuric ions. *Nanoscale* **2014**, *6* (8), 4096-101.

72.   Wang, G.; Yau, S.; Mantey, K.; Nayfeh, M. H., Fluorescent Si nanoparticle-based electrode for sensing biomedical substances. *Optics Communications* **2008**, *281* (7), 1765-1770.

73.   Shiqi, J.; Zifan, L.; Tiantian, S.; Yanting, F.; Chunxia, Z.; Pengzhi, H.; Shengli, S.; Chengyong, L., High Sensitivity Detection of Copper Ions in Oysters Based on the Fluorescence Property of Cadmium Selenide Quantum Dots. *Chemosensors* **2019,** *7* (4), 47.

74.   Xie, H.; Liang, J.; Zhan, Z.; Liu, Y.; He, Z.; Pang, D., Luminescent CdSe-ZnS quantum dots as selective Cu2+ probe. *Spectrochimica Acta Part A: Molecular and Biomolecular Spectroscopy* **2004,** *60* (11), 2527-2530.

75.   Wang, A.; Fu, L.; Rao, T.; Cai, W.; Yuen, M.; Zhong, J., Effect of metal ions on the quenching of photoluminescent CdTe QDs and their recovery. *Optical Materials* **2015,** *42*, 548-552.

76.   Passos, S. G. B.; Kunst, T. H.; Freitas, D. V.; Navarro, M., Paired electrosynthesis of ZnSe/ZnS quantum dots and Cu^{2+} detection by fluorescence quenching. *Journal of Luminescence* **2020,** *228*, 117611.

77.   Zhu, B.; Tang, M.; Yu, L.; Qu, Y.; Chai, F.; Chen, L.; Wu, H., Silicon nanoparticles: fluorescent, colorimetric and gel membrane multiple detection of Cu^{2+} and Mn^{2+} as well as rapid visualization of latent fingerprints. *Analytical Methods* **2019,** *11* (28), 3570-3577.

78.   Jin, L. H.; Han, C. S., Ultrasensitive and selective fluorimetric detection of copper ions using thiosulfate-involved quantum dots. *Anal Chem* **2014,** *86* (15), 7209-13.

79.   Peng, C.; Zhang, Y.; Qian, Z.; Xie, Z., Fluorescence sensor based on glutathione capped CdTe QDs for detection of Cr 3+ ions in vitamins. *Food Science and Human Wellness* **2018,** *7* (1), 71-76.

80.   Nguyen, A.; Gonzalez, C. M.; Sinelnikov, R.; Newman, W.; Sun, S.; Lockwood, R.; Veinot, J. G.; Meldrum, A., Detection of nitroaromatics in the solid, solution, and vapor phases using silicon quantum dot sensors. *Nanotechnology* **2016,** *27* (10), 105501.

81.   Yi, Y.; Deng, J.; Zhang, Y.; Li, H.; Yao, S., Label-free Si quantum dots as photoluminescence probes for glucose detection. *Chem Commun (Camb)* **2013,** *49* (6), 612-4.

82.   Bisaglia, M.; Bubacco, L., Copper Ions and Parkinson's Disease: Why Is Homeostasis So Relevant? *Biomolecules* **2020,** *10* (2), 195.

83.   Purchase, R., The Link between Copper and Wilson's Disease. *Science Progress* **2013,** *96* (3), 213-223.

84.   Somers, R. C.; Bawendi, M. G.; Nocera, D. G., CdSe nanocrystal based chem-/bio-sensors. *Chem Soc Rev* **2007,** *36* (4), 579-91.

85.   Knowles, K. E.; Hartstein, K. H.; Kilburn, T. B.; Marchioro, A.; Nelson, H. D.; Whitham, P. J.; Gamelin, D. R., Luminescent Colloidal Semiconductor Nanocrystals Containing Copper: Synthesis, Photophysics, and Applications. *Chem. Rev.* **2016**.

86.   Hoffman, R. M., Cell Markers: Green Fluorescent Protein. **2013**, 483-487.

87.   Hildebrandt, N.; Spillmann, C. M.; Algar, W. R.; Pons, T.; Stewart, M. H.; Oh, E.; Susumu, K.; Díaz, S. A.; Delehanty, J. B.; Medintz, I. L., Energy Transfer with Semiconductor Quantum Dot Bioconjugates: A Versatile Platform for Biosensing, Energy Harvesting, and Other Developing Applications. *Chemical Reviews* **2017,** *117* (2), 536-711.

88.   Kagan, C. R.; Murray, C. B.; Nirmal, M.; Bawendi, M. G., Electronic Energy Transfer in CdSe Quantum Dot Solids. *Physical Review Letters* **1996,** *76* (9), 1517-1520.

89.   Kagan, C. R.; Murray, C. B.; Bawendi, M. G., Long-range resonance transfer of electronic excitations in close-packed CdSe quantum-dot solids. *Physical Review B* **1996,** *54* (12), 8633-8643.

VITA

NAME   Nattakarn Phromsiri

DATE OF BIRTH   01 November 1992

PLACE OF BIRTH   Bangkok

INSTITUTIONS ATTENDED   B.Sc. Chulalongkorn university

HOME ADDRESS   333/29 SYM condo vibhavadi, Chomphon, Chatuchak, BKK
                         10900